Aus dem CharitéCentrum 6 für Diagnostische und Interventionelle Radiologie und Nuklearmedizin, Klinik für Radiologie mit den Bereichen Kinderradiologie und Neuroradiologie

Direktor: Professor Dr. med. Bernd Hamm

Habilitationsschrift

Klinische Translation quantitativer MRT Verfahren in der Neuroradiologie

(Clinical translation of quantitative MRI techniques in Neuroradiology)

zur Erlangung der Lehrbefähigung für das Fach Radiologie

vorgelegt dem Fakultätsrat der Medizinischen Fakultät Charité-Universitätsmedizin Berlin

von

Dr. med. Anna Tietze, PhD

Eingereicht: September 2021
Dekan: Professor Dr. med. Axel R. Pries
1. Gutachter: Prof. Dr. med. Elke Hattingen, Universitätsklinikum Frankfurt, Göthe Universität
2. Gutachter: Prof. Dr. med. Thomas Liebig, Ludwig-Maximilian-Universität München

Contents

Acronyms

2CXM 2-compartment-exchange model. 15, 16, 51, 52, 67, 68, 113, 123

2HG 2-hydroxyglutarate. 12, 13, 41, 42, 110, 112, 113, 122

APT Amide Proton Transfer. 9, 10, 11, 21, 22, 35, 110, 112, 116, 121, 122, 124

BM Bayesian method. 51, 52, 67, 68, 113, 114, 123, 124

CBF cerebral blood flow. 16

CBV cerebral blood volume. 15, 16

CEST Chemical Exchange Saturation Transfer. 10, 22

CM1 Chiari malformation type 1. 16, 86, 116

CM2 Chiari malformation type 2. 16, 86, 116

CNS central nervous system. 12, 19, 42, 67, 114, 115, 120, 121, 122, 123

CSD cortical spreading depression. 35, 116, 122

CSF cerebrospinal fluid. 10, 16, 17, 22, 86, 87, 110, 122

DCE Dynamic Contrast Enhanced. 9, 13, 14, 15, 16, 51, 52, 67, 113, 114, 116, 119, 123

DSC Dynamic Susceptibility Contrast. 13, 14, 15, 16, 51

ETM extended Toft's model. 15, 51, 52, 67, 68, 123

F_p plasma flow. 16, 52, 68

FFE Fast Field Echo. 16

FHM Familial hemiplegic migraine. 35, 116, 122

FIESTA Fast Imaging employing steady-state acquisition. 16

FISP Fast Imaging with steady-state free precesion. 16

GBM glioblastoma multiforme. 13, 15, 67, 68

IDH Isocitrate Dehydrogenase. 12, 13, 41, 42, 110, 112, 113, 122

K_1 permeability rate. 16, 52, 113

K_{trans} volume transfer constant. 15, 16, 52, 113, 119, 123

LM Levenberg-Marquardt. 51, 67, 68, 114, 123

MP2RAGE magnetization-prepared rapid gradient echo with two inversion times. 18, 96, 97, 115, 117, 119, 123

MPRAGE magnetization-prepared rapid gradient echo. 17, 18, 86

MRI Magnetic Resonance Imaging. 8

MRS Magnetic Resonance Spectroscopy. 9, 11, 12, 13, 41, 42, 110, 112, 113, 122

PCR polymerase chain reaction. 13, 42

PRESS point-resolved spectroscopy. 41

qMRI Quantitative Magnetic Resonance Imaging. 8, 9, 18, 109, 113, 117, 118, 119, 120, 121, 123

STEAM stimulated echo acquisition mode. 41

T2FLAIR T2-weighted fluid attenuated inversion recovery. 22, 52

$\mathbf{V}_e$ extravascular-extracellular space. 15, 52, 67, 68, 113

$\mathbf{V}_p$ plasma volume. 15, 16, 52, 123

VIDM voxel intensity distribution method. 87, 120, 122

WHO World Health Organization. 12, 113, 122

Chapter 1

Introduction

1.1 General Aspects of quantitative Magnetic Resonance Imaging in Neuroimaging

The collection of quantitative information in Magnetic Resonance Imaging (MRI) data is an immense field of research providing imaging biomarkers that describe anatomy and biological function and help to understand pathophysiology in a wide range of diseases. Depending on the underlying MRI technique and the subsequent post-processing of the imaging data a variety of metric quantities can be calculated in each individual voxel, the subunit of reconstructed MRI data. By modelling or direct interpretation of metrics, parameter maps are generated and can be used to describe tissue microstructures, e.g. cell density or the composition of the intra-/extracellular matrix [1, 2] or physiological parameters, such as perfusion or metabolism [3–7]. It is obvious that the understanding of anatomy, physiology, and function is an indispensable premise to recognise and comprehend any pathological condition, with tumour [8–10], vascular [11, 12], infectious [13], or neurodegenerative diseases [14] serving only as examples.

Undoubtedly, Quantitative Magnetic Resonance Imaging (qMRI) has found its way into the clinical routine to a certain extent, but is still enormously underrepresented compared to the immense knowledge gained in research during the last three centuries. Broadly speaking, qMRI stands in contrast

to the qualitative assessment of MRI data that is primarily done in the clinical context today. While the benefit of qualitative MRI is of no doubt and has advanced diagnostics, the understanding of diseases, and the effect of different treatment strategies immensely, its main disadvantage is that the MRI signal intensity is relative and, thus, not quantitatively comparable between patients, MRI systems, or time points. This is due to the fact that the MRI signal is influenced by local intensities and contrasts that are a complicated interplay of MRI acquisition parameters and hardware dependent issues, which include system imperfections of the static magnetic or the radiofrequency field as well as the quality of the receiver coils, to mention just a few. Particularly in multicenter studies, this can lead to inhomogeneous inclusion or outcome criteria and compromises are likely to influence study results in the end.

Why is the clinical adoption of qMRI so hesitant? If these techniques really are useful in the clinical context and might increase reproducibility and objectivity, where are the barriers to translate them? Obstacles are surely diverse and include misunderstandings between clinical users and basic researchers, technical requirements that are difficult to accommodate in a clinical environment, validation issues, and the need of multidisciplinary teams, where the applicability can be discussed.

In the following, five examples of qMRI techniques predominantly developed in basic neuroscience are shortly described. Specifically, Amide Proton Transfer (APT), quantitative Magnetic Resonance Spectroscopy (MRS), the perfusion-weighted MRI technique Dynamic Contrast Enhanced (DCE) MRI, quantitative assessment of CINE MRI, and a T1 mapping technique are explained. In the second part of this thesis, these techniques are applied in four disease entities (ischaemic stroke, migraine, primary brain tumours, and brain malformations) as well as in the imaging-based maturation assessment of infants and young children.

1.2 Examples of quantitative MRI techniques in Neuroradiology

1.2.1 pH-weighted Amide Proton Transfer (APT) Chemical Exchange Saturation Transfer (CEST) MRI

APT imaging belongs to a more general technique termed Chemical Exchange Saturation Transfer (CEST), where a radiofrequency pulse is given with a certain, non-water specific frequency leading to energy absorption in solute molecules. In APT imaging this "off-resonance" pulse specifically targets the protons of endogenous amides, nitrogen-containing compounds that are primarily found at the backbone of proteins *in vivo*. Through intermolecular saturation (mostly proton exchange and cross-relaxation), the energy is subsequently transferred to the water resonance, which is reflected in altered signal intensities. The APT effect is slighly different for grey and white matter and cerebrospinal fluid (CSF), eliciting the contrast on parameter maps.

The proton exchange effects are influenced by temperature and tissue pH. The temperature is assumed to be relatively stable *in vivo*, but as the proton exchange rate is a base-catalyzed process, tissue acidosis leads to a reduction of the APT effect size. Therefore, APT imaging can be regarded as a pH-weighted imaging method.

APT imaging has been applied in glioma patients showing APT hyperintensity in high grade glioma [15]. Although counterintuitive at first glance, because the anaerobic glycolysis should lead to an acidic environment and a decreasing APT effect, the APT hyperintensity is assumed to be related to the high intracellular protein concentration in tumour cells as well as the increased protein content due to tumour neo-angiogenesis. APT imaging is therefore suitable for non-invasive brain tumour grading and allows targeted biopsies by direct visualization of high-grade regions within heterogeneous glioma [16].

The pH-sensitivity of APT imaging appears especially suitable for the detection of anaerobic metabolism in ischaemic tissue. This was shown for the first time in a rat ischaemia model [17] and subsequently in single patients with subacute ischaemic strokes (1 to 7 days after symptom onset) [18].

APT imaging has recently been introduced on commercially available MRI systems, which will without doubt result in future fields of application [15].

1.2.2 Quantitative Proton Magnetic Resonance Spectroscopy (MRS)

MRS is a well established technique to determine the presence and relative concentration of different metabolites in tissue *in vivo*. Although today MRS can be performed on most clinical MRI systems, the acceptance within the community is still relatively low. The reason may lie in its low specificity when used non-critically in too general questions, in its low resolution, the increased susceptibility for image artefacts, and the merely semi-quantitative approach used in many studies. MRS fascinates, however, by its simple implementation in clinical imaging protocols and the potential to explore tissue for metabolic changes.

In clinical MRS mostly proton spectra are acquired, i.e. the resonance frequency of protons in different chemical environments are detected. The resonance frequency f is determined by the magnetic field B_0 and the gyromagnetic ratio (42.58 MHz/Tesla for protons) as defined by the Larmor equation:

$$f = B_0 \cdot \gamma \tag{1.1}$$

Protons experience, however, a modified, local B_0, depending on their chemical neighbours that through their characteristic electron clouds oppose the main B_0. This very small change of f allows to analyse the molecular composition of tissue by determining the chemical shift for protons in different molecular configurations. Obviously, the concentration of protons bound by water in brain tissue outplays that of any other molecule and would reduce the peaks of other metabolites beyond detection, why water suppression sequences must be applied.

The size and the shape of a metabolite peak is among other things influenced by its concentration, but it is important to keep in mind that the peak height and shape depend on the amount of active protons and not on the molar concentration alone as well as on T1 and T2 effects. In general, signal ratios of metabolites, e.g. N-acetyl aspartate to creatine, are used for semi-quantification. This allows for a certain inter- and intraindivdual comparison. Absolute concentrations can be achieved

by calibration procedures [19], which is mostly not practical in a clinical context, why water is usually used as an internal reference [20]. For this purpose, an additional acquisition without water suppression is done and metabolite concentration is calculated assuming a water content of approx. 47 mM.

Clinical MRS in the brain is used for various pathologies, mostly for brain tumours, but with the exception of few diseases, e.g. creatine synthesis defects or Canavan disease, MRS is, however, relatively non-specific and often serves only as a supportive tool in otherwise qualitative assessment.

A recently described exception is the detection of 2-hydroxyglutarate (2HG), a metabolite that is normally not produced in brain tissue, but is existent in gliomas with Isocitrate Dehydrogenase (IDH) mutations. In the following, the significance of the IDH mutational status is shortly explained in order to illustrate the clinical importance of this method and how it can contribute considerably to presurgical, non-invasive diagnostics and serve as an imaging biomarker for disease progression or treatment response [21].

The significance of Isocitrate Dehydrogenase (IDH) mutations in glioma

Since the publication of the revised World Health Organization (WHO) classification of central nervous system (CNS) tumours in 2016, the approach to primary brain tumours has been revolutionised [22]. The gain in experience since the 2007 version of the WHO classification scheme had led to the insight that the consideration of molecular biomarkers enables a more precise classification, that additional tumour entities can be defined, and that the patient outcome can possibly be improved by using targeted therapies.

Gliomas originate from neuroepithelial cells and are divided in astrocytomas and oligodendrogliomas. In the 2007 WHO classification, this was achieved by histological diagnosis alone, which can be difficult. It is obvious that unclear classification has profound consequences for outcome prediction and treatment choice. Numerous molecular markers have been integrated into the 2016 WHO classification allowing a meaningful reclassification of most entities.

The mutational status of the IDH gene is one key factor dividing glioma in two prognostic groups, which already was described in 2009 by Yan et al. [23]. Here, it was shown that IDH mutations were present in 85% of secondary glioblastoma multiforme (GBM), i.e. from lower grades (grade II or III) transformed tumours, whereas they were rare in primary GBMs, i.e. in patients without a precursor glioma (5%). In addition, 73% of astrocytoma grade III and 90% of patients with astrocytoma grade II had IDH mutations. In this study, a striking difference of survival times for patients with astrocytoma grade III and GBMs with and without IDH mutations was found with IDH wildtype tumours showing significantly shorter survival times [23]. This study only confirms what clinical experience already had proven; the histological diagnosis is only part of the full picture and molecular markers, not only the IDH mutational status, have considerable impact on patient outcome.

The usual diagnostic workup for assessing the IDH mutational status is immunohistochemistry or polymerase chain reaction (PCR), both obviously requiring tumour tissue. In 2012, Choi et al. described for the first time that the IDH mutational status can be determined by MRS and showed a high diagnostic accuracy with 100% specificity and sensitivity in 35 patients [24]. The biochemical basis for the detection of IDH mutations by MRS is a gain of function that generates 2HG, which is normally not produced. This is illustrated in Fig. 1.1 depicting the citric acid cycle. There are different types of IDH, where type 1 and 2 are of importance for tumour diagnostics. IDH type 1 is cytosolic (light blue background in Fig. 1.1), whereas type 2 is localised in the mitochondrial matrix (grey background in Fig. 1.1). Interruption of the metabolic pathway due to a IDH mutation irrespective of type leads to an accumulation of 2HG that then can be detected by a dedicated MRS sequence.

1.2.3 Perfusion-weighted MRI with gadolinium contrast agents

Contrast-based perfusion-weighted MRI encompasses two methods; the T2-weighted Dynamic Susceptibility Contrast (DSC) and the T1-weighted DCE technique. Both techniques can be used to measure various perfusion parameters by following a bolus of gadolinium contrast agent through the vascular system. The first pass of the contrast agent is detected by fast, repeated imaging of the dedicated region. Numerous post-processing approaches to calculate haemodynamic parameters are described (for an

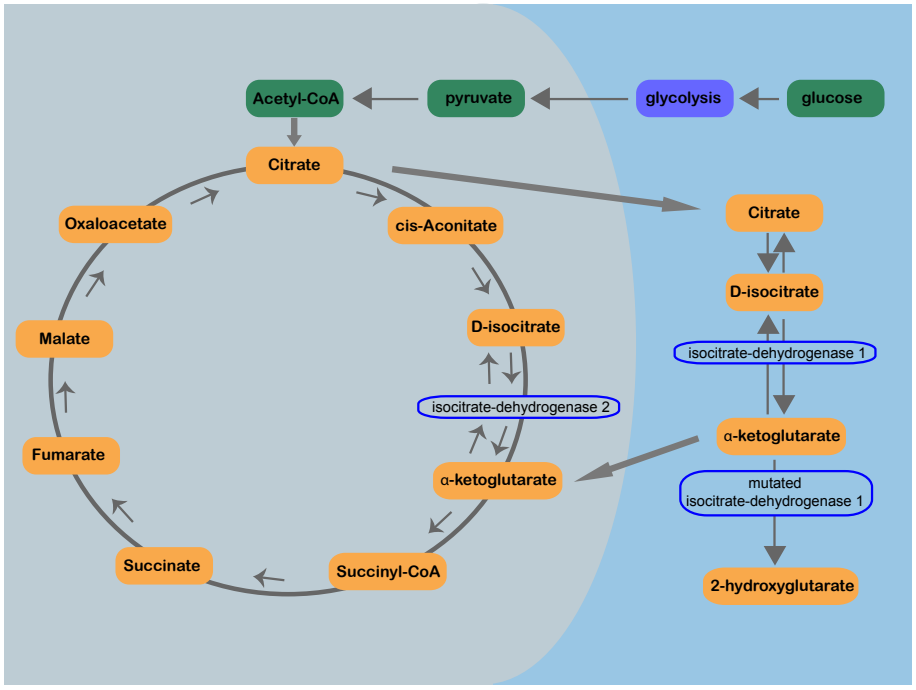

Figure 1.1: The citric acid cycle and the function of isocitrate dehydrogenase (IDH). **I**DH is an enzyme of the citric acid cycle that is located in the mitochondrial matrix (schematised with grey background) and the cytosol (light blue background). Mutations in either the IDH type 1 or type 2 gene leads to an accumulation of 2-hydroxyglutarate (2HG) by interruption of the metabolic pathway.

overview see [25] and [26]). Broadly speaking, model-independent, model-based, and statistical methods can be applied, each with its advantages and disadvantages.

While DSC is widely-used in the clinical context, e.g. for stroke and tumour patients, as well as in trials and research, DCE has so far only been able to assert itself with difficulties in the field of neuroscience and clinical brain imaging. The advantage of DCE is, however, a better image resolution, absolute parameter quantification (in DSC values are relative), and the possibility to generate additional metrics that allow the calculation of blood-brain-barrier permeability indices. In fact, a defective blood-brain-barrier poses a problem for DSC, as the parameter calculations are incorrect in the presence of contrast leakage [27]. In addition, blood products, whether as a result of surgery or spontaneous hemorrhages, cause considerable susceptibility artefacts that in the worst case make calculated DSC maps non-diagnostic.

Perfusion parameters in cerebral gliomas

DSC MRI has found broad acceptance in brain tumour diagnostics for the *in vivo* evaluation of neoangiogenesis, i.e. the development of new vessels. The first study to explore perfusion-weighted MRI to investigate tumour vascularity was performed in the early nineties [28], where significantly higher cerebral blood volume (CBV) in high-grade than low-grade glioma was found. This is illustrated in Fig. 1.2, where high CBV is represented by red and orange colours and low by blue (right side). Fig. 1.2 A shows a low-grade, Fig. 1.2 B a high-grade glioma (left side: T1-weighted contrast-enhanced image, CE T1; right side CBV map). Very high CBV values are present in the enhancing rim around the necrotic centre of the left frontal GBM (Fig. 1.2 B). Even the small satellite tumour in the left corona radiata stands out due to its high values. For comparison the astrocytoma grade II in Fig. 1.2 A shows very low CBV.

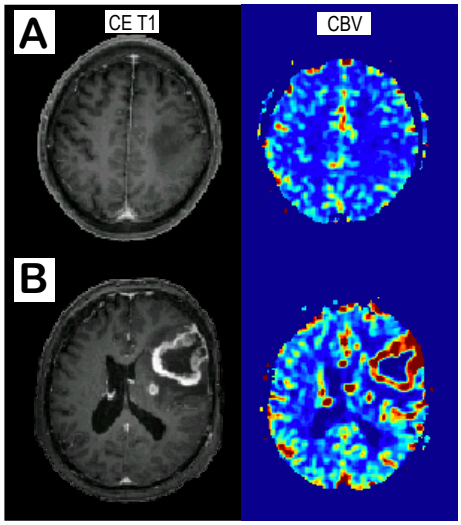

Figure 1.2: (A) Left: T1-weighted, contrast enhanced image (CE T1) of an astrocytoma grade II (left corona radiata). Right: Cerebral blood volume (CBV) map with for low-grade glioma typical decreased values. (B) Corresponding images of a Glioblastoma multiforme with very high CBV values en the contrast enhancing part of the tumour.

An abundance of studies have been published since, investigating different haemodynamic parameters and perfusion techniques to diagnose tumour type and grade, treatment response, recurrence, progression, or treatment-related tissue changes [10, 29]. Most of these studies are based on the more established DSC, for which commercial analysis software is available.

Most DCE studies in brain imaging use model-based approaches, often the extended Toft's model (ETM) [30] or the 2-compartment-exchange model (2CXM) [31, 32]. The ETM enables the calculation of parameters describing the blood-brain-barrier (volume transfer constant (K_{trans}), extravascular-extracellular space (V_e)) and the plasma volume plasma volume (V_p). The 2CXM allows moreover the separation of K_{trans} into the

permeability rate permeability rate (K_1) and the flow-dependent blood supply, here termed plasma flow (F_p). This separation is valuable in tumours, since changes of blood flow and permeability do not have to run parallel and might provide different information. The blood supply and permeability V_p and F_p are more or less following results obtained by DSC, as they relate very closely to CBV and cerebral blood flow (CBF). In addition, K_{trans} and K_1 allow reliable distinction between high- and low-grade glioma as well as between tumour recurrence and treatment-related changes [33].

Despite the aforementioned advantages of DCE imaging, the clinical adoption is relatively hesitant. The causes might be the variability of results, as parameter values depend on the sequence, the postprocessing procedure [34, 35], and the underlying model [36]. It also has to be kept in mind that the parameter estimation in more complex models as for example the 2CXM can lead to less reliable values, making the parametric maps rather noisy and in the end non-diagnostic.

1.2.4 Quantification of movement on dynamic CINE MRT

Dynamic MRI is a technique to real-time visualise moving structures. e.g. cardiac or swallowing function, fetal motor behaviour, or bowel movements [37–40]. Usually a cardiac- or pulse-gated balanced steady-state free precession MRI sequence is used, e.g. true Fast Imaging with steady-state free precesion (FISP), Fast Imaging employing steady-state acquisition (FIESTA), or balanced Fast Field Echo (FFE), and a cine loop is captured, why this technique is generally termed CINE MRI.

In neuroimaging, CINE MRI can be applied to investigate pulsatility dependent movement, which has mostly been done in patients with Chiari malformations [41–43]. In these malformations, anomalies of the cranial base and vault result in overcrowding of posterior fossa structures. The Chiari malformation type 1 (CM1) is relatively common [44], and symptoms as neck pain and headache occur due to brain stem and/or cerebellar compression. The Chiari malformation type 2 (CM2) is much rarer. The underlying malformation of the CM2 is a neural tube defect leading to disturbed CSF passage and CSF leakage that results in insufficient bone development, a too small posterior fossa, and subsequent underdevelopment of the hindbrain. The accompanying open spinal dysraphisms makes

the patients symptomatic already in the neonatal period. Various symptoms can occur due to the often severe compression of the brainstem and the upper cervical spinal cord as well as the hydrocephalus. The Chiari malformation type 3 is the rarest of the three types and characterised by a bony defect at the cranio-cervical junction with a concomitant myelomeningocele at this level.

CINE MRI in these patients is usually evaluated qualitatively, i.e. the pulsatility dependent tissue compression is merely observed and at the most semi-quantitatively described, which makes reproducibility and inter-/intraindividual comparison an issue [41, 42]. The importance of CINE MRI as part of the imaging protocols lies in the recognition of a potentially dynamic herniation of the cerebellar tonsils and the visualisation of only intermittent brainstem compression as well as CSF disturbances.

1.2.5 T1 mapping using the Magnetization Prepared 2 Rapid Acquisition Gradient Echoes (MP2RAGE) sequence

T1 and T2 relaxation is among other parameters an important source of MRI contrast and is encoded as signal intensities in arbitrary units in the imaging voxel. In the clinical context, the exact T1 and T2 values are mostly disregarded and instead, T1- and T2-weighted images are used. Weighting implies that different tissue parameters, i.e. T1, T2, spin density, diffusion, susceptibility etc. contribute together to the image contrast. Mapping techniques, on the other hand, allow the voxelwise quantification of single parameters, e.g. T1 and T2 relaxation time in s, that can be presented as parametric maps and are an indispensable tool to measure small variations across time and space.

The T1 relaxation is the regrowth of the longitudinal magnetisation after the application of the radiofrequency pulse that tips the spins out of the longitudinal alignment. T1 is the time needed to return to the point of origin. Different techniques for T1 mapping have been described, usually implying the acquisition of several sets of data, either as separate acquisitions or in one sequence (for an overview see [45]).

Recently a new MRI sequence has been developed for improved tissue segmentation and T1 mapping [46]. This sequence is based on the very commonly used magnetization-prepared rapid gradient echo (MPRAGE)

sequence, which provides high resolution T1-weighted images. By adding two inversion times to the MPRAGE (usually referred to as TI_1 and TI_2) images are generated that are free of inhomogeneities by the radiofrequency field and T2* effects. The sequence is known as magnetization-prepared rapid gradient echo with two inversion times (MP2RAGE).

While existing T1 mapping approaches have in common that additional acquisitions have to be made, the MP2RAGE can be used for diagnostic purposes and as T1 mapping method at the same time. This time savings is particularly attractive in the area of paediatric imaging, as this patient group is less likely to cooperate and anaesthesia time should be kept as short as possible.

T1 is known to change rapidly in infants and young children due to the development and maturation of myelin, why T1 mapping methods to quantify myelin have been described [47–50]. The main function of myelin sheaths is to insulate axons in order to increase the speed of electric pulses and thereby the nerve conduction velocity. The development of myelin sheaths is an important step of brain maturation that continues well into adulthood. The assessment of myelination is an integral part of imaging diagnostics in children, because delayed or even accelerated myelination can be a sign of various diseases [51].

In the clinical context, myelination is usually assessed qualitatively on conventional T1- and T2-weighted images, where mature myelin becomes T1 hyper- and T2 hypointense. This is illustrated in Fig. 1.3, where the infant aged 208 days has developed myelin in the posterior limb of the internal capsule and the splenium (orange arrows) and to a minor degree in the periventricular white matter. In the older child, aged 1482 days, T2 hypo-/T1 hyperintense myelin is visible in the entire white matter of these slices. The timing and spatial distribution of mature myelin in the young, healthy brain follows a fixed pattern, which requires a not insignificant experience to recognise reliably. Pictorial atlantes and textbooks, partially available online, help to accomplish this (as an example `https://www.myelinationmriatlas.com/`, accessed 01/03/2021).

1.3 Aim and outline of the present work

The main purpose of this work is to translate advanced qMRI techniques into the clinical setting. The hypothesis is that conventional and pri-

marily qualitative imaging assessment can be strengthened by quantitative information through greater reproducibility and additional anatomic, metabolic, or functional data.

The translation of advanced techniques is, however, not always straightforward and the assessment of feasibility, usefulness, and robustness are an important step when moving new approaches from "bench to bedside". The data acquisition procedures and the post-processing workflow have to be adapted to the clinical environment, where critically ill patients, time constrains, and an efficient use of health care resources require pragmatism and compromises. Clinical translation of advanced MRI biomarkers is inevitably a delicate balance between these clinical needs and limitations on the one hand and the technical challenges that can go along with the introduction of novel MRI techniques and post-processing methods on the other hand. At the same time, the evidence and informative value of the biomarkers must under no circumstances be compromised by the necessary technical modifications.

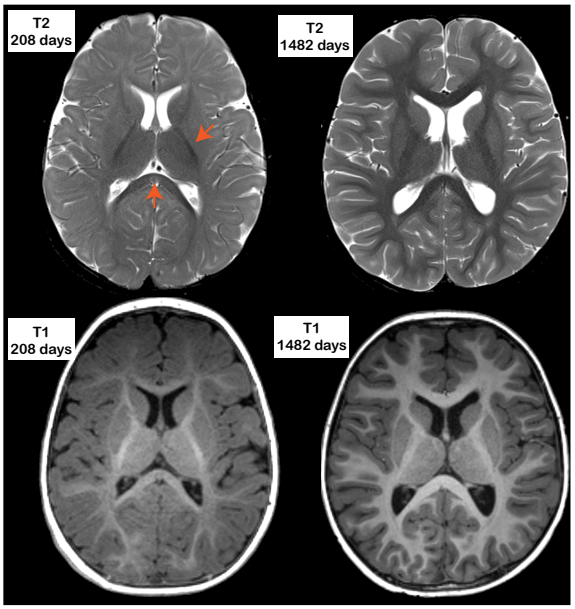

Figure 1.3: T2-weighted (upper row) and T1-weighted (lower row) images of a child aged 208 days (left) and 1482 days (right), respectively. Mature myelin is hypointense on T2-weighted and hyperintense on T1-weighted images compared cortical grey matter, e.g. in the posterior limb of the internal capsule and in the splenium (orange arrows) in the younger child.

In this work, the gap between research and clinical practice is addressed by presenting and evaluating five quantitative MRI methods in the context of four CNS pathologies as well as in the quantitative description of brain maturation. Some techniques were newly developed and some were pre-existing but further developed. The overall aim is to bridge this gap and to enhance the acceptance of new approaches in the clinical community.

In the following, different stages of clinical translation are presented: (i) Entirely new methods are described or moved from phantom or animal

studies to small cohorts of healthy subjects or patients (**study 1**, **study 2**, and **study 6**). Here, potential technical challenges and focus areas for further development are identified. (ii) Results that have been achieved in research labs and tested on single clinical departments have to be replicated in different clinical setting for evaluating reproducibility and robustness of new techniques (**study 3** and **study 7**). (iii) After identifying potential problems and pitfalls of new MRI techniques or postprocessing approaches, optimisation procedures must be proposed and tested. Here it is of essential importance that accuracy and precision are maintained or improved, once again balancing clinical and research requirements (**study 4** and **study 5**).

Chapter 2

Own publications

Study 1 and **study 2** represent very early stages of clinical translation. A recently developed ph-weighted APT imaging technique was moved from a preclinical to a clinical environment. It had been designed in phantoms, tested in healthy subjects, and small patient cohorts and was now for the first time applied in patients with acute stroke and familial hemiplegic migraine to detect anaerobic glycolysis and subsequent tissue acidosis *in vivo*. The aim was to investigate feasibility and usefulness in the acute and subacute setting.

2.1 Assessment of ischaemic penumbra in patients with hyperacute stroke using amide proton transfer (APT) chemical exchange saturation transfer (CEST) MRI

Anna Tietze, Jakob Blicher, Irene Klærke Mikkelsen, Leif Østergaard, Megan K. Stroher, Seth A. Smith, Manus J. Donahue

NMR in Biomedicine 2014 Feb; 27(2): 163-174
https://doi.org/10.1002/nbm.3048

In the state of hypoxia the metabolism changes from aerobic to anaerobic glycolysis leading to tissue acidosis. In cerebral ischaemia, the infarct core consists of irreversibly damaged tissue that is surrounded by the ischaemic penumbra, hypoperfused regions at risk that can be rescued by treatment. It has been shown that the penumbra includes areas of benign oligaemia that can survive without recanalisation [52]. This prospective study was

the first to use APT imaging, a pH-weighted CEST imaging technique, in hyperacute stroke patients with the aim to delineate tissue at risk more precisely.

APT imaging was established on a clinical 3T Philips Achieva 3TX system (Philips Medical Systems, Best, Netherlands) on five healthy subjects to ensure correct parameter setting and adequate contrast in different tissue types. Since a time saving is pivotal in acute stroke patients, the APT sequence had to be modified. To investigate if sufficient APT contrast still was present with these scan parameters simulations at different pH values were performed. All postprocessing and simulations were done using Matlab (Mathworks, Natick, MA, USA). Ten patients with acute stroke symptoms (7 with symptom onset < 4 hours, $3 < 24$ hours) were imaged using conventional MRI sequences, diffusion- and perfusion-weighted MRI as well as APT. The scan duration for the entire protocol was 10 min 52 s, including 3 min 20 s for the APT imaging sequence. The APT index was calculated in the diffusion-restricted regions, i.e. the core, in the penumbra (time-to-peak lengthening on perfusion-weighted MRI), and in the final infarct (defined on follow-up T2-weighted fluid attenuated inversion recovery (T2FLAIR) MRI).

The APT contrast was good for healthy grey and white matter as well as for CSF for our protocol. Simulations proved that the APT effect decreased with lower pH as expected. The APT effect size in ischaemic regions was significantly smaller compared to normal white matter (p=0.03). A trend (p=0.10) for an APT reduction averaged over all ten patients could be shown comparing the final infarct volume and the region with time-to-peak lengthening. Owing to the small number of included patients with relatively heterogeneous clinical conditions regarding stroke location, extent of penumbra, and treatment, statistically valid conclusions could not be expected. Nevertheless, it could be shown that the APT effect size correlated with final infarct volume on case-by-case comparison.

This study was foremost a proof of concept for clinical APT imaging. The focus was therefore primarily on the identification of pitfalls and technical limitations in order to be able to address them for future development. Especially for stroke imaging, rapid, low-power, motion-desensitised techniques are necessary.

2.2 Perfusion and pH MRI in familial hemiplegic migraine with prolonged aura

Jakob Udby Blicher, Anna Tietze, Manus J. Donahue,
Seth A. Smith, Leif Østergaard

Cephalalgia 2016 Mar; 36(3): 279-283
https://doi.org/10.1177/0333102415586064

Familial hemiplegic migraine (FHM) is a rare type of migraine with motor weakness as aura manifestation that may be accompanied headaches, epileptic seizures, and in some cases progressive brain atrophy. In most patients, an autosomal dominant inheritance pattern is observed, and a first-degree relative with identical migraine symptoms is required as one of the diagnostic criteria. FHM belongs to the ion-channelopathies, i.e. missense mutations lead to compromised functions of ion channels, e.g. the Na^+/K^+-ATPase in the membrane of glia cells [53, 54]. As in common migraine, the aura i thought to be the result of spontaneous neuronal activity that migrates over the cortex and is followed by a more or less lasting neuronal inhibition, a phenomenon termed cortical spreading depression (CSD) [55].

The aim of this study was to shed some light on the metabolic changes during the aura and CSD, respectively. The hypothesis was that capillary flow disturbances as the starting trigger can give rise to tissue hypoxia and acidosis without leading to ischaemia and that this constellation entails CSD. Tissue hypoxia was indirectly deducted by using perfusion-weighted MRI and a well-described model [7], whereas acidosis was detected by APT and ischaemia by diffusion-weighted MRI. A 44-year old patient with aura symptoms from the left hemisphere including aphasia was imaged twice during his prolonged aura. The acute MRI showed distinct capillary low disturbances indicating tissue hypoxia without diffusion restriction that otherwise would be in keeping with ischaemia. On his second MRI on day 12 of his aura, he had developed diffuse cortical vasogenic oedema and a considerable increase of APT asymmetry signal highly suggestive of acidosis following anaerobic glycolysis. Although none of the techniques can prove or disprove CSD in this patient, this was the first study to employ APT MRI in migraine and specifically in a FHM patient.

Study 3 is an example of a reproducibility study. Replication of research results by a different team and in a different clinical setting are highly relevant for the acceptance and implementation of new techniques. In this study, the 2HG MRS sequence was modified to ensure that the total imaging time of brain tumour patients did not exceed 30 min. After this technique had been tested in smaller cohorts of glioma patients in a research environment it should be determined if a similar diagnostic accuracy could be achieved in a clinical setting and if 2HG MRS can contribute to patient management.

2.3 Noninvasive assessment of isocitrate dehydrogenase mutation status in cerebral gliomas by magnetic resonance spectroscopy in a clinical setting

Anna Tietze, Changho Choi, Bruce Mickey, Elizabeth A. Maher, Benedicte Parm Ulhøi, Ryan Sangill, Yasmin Lassen-Ramshad, Slavka Lukacova, Leif Østergaard, Gorm von Oettingen

J Neurosurg 2017 Feb; 128(2): 391-398
https://doi.org/10.3171/2016.10.JNS161793

The diagnostic and prognostic relevance of mutations in the IDH gene for glioma patients is today beyond doubt. It has recently been described by Choi et al. that the metabolite 2HG that is exclusively produced in IDH-mutated cells can be detected *in vivo* by MRS [24]. The aim of this study was to translate the technique from a research lab to a clinical environment and to investigate if quantitative 2HG-MRS can be integrated into diagnostic imaging protocols for glioma patients.

Thirty-five treatment-naïve patients suspected for glioma were included into this prospective study. Imaging was performed on a 3T Philips Achieva 3TX system (Philips Medical Systems, Best, Netherlands). A sin-gle voxel ($2\times2\times2$ cm^3), optimised point-resolved spectroscopy (PRESS) sequence was added to the standard brain tumour MRI protocol extend-ing the examination time by 4 min 22 s. To quantify metabolites, an unsuppressed water signal was measured with a stimulated echo acquisi-tion mode (STEAM) sequence (40 s). Data were post-processed offline using Matlab (Mathworks, Natick, MA, USA) and LCModel (accessed 01/03/2021: `http://s-provencher.com/lcmodel.shtml`). This took approximately 2 min. Targeted biopsies were taken from the voxel to

ensure correlation between 2HG MRS and results obtained by immunohistochemistry and/or PCR. Receiver operating characteristic curves were generated using R (Boston, MA, USA).

After biopsy or resection, 30 glioma cases, one case of a gangliocytoma, and one case of a CNS lymphoma was diagnosed. One case showed non-specific, inflammatory cells, one patient was diagnosed with tumefactive multiple sclerosis, and the last case with autoimmune encephalitis.

2HG MRS diagnosed IDH mutational status correctly in 31 of 35 cases with two false negatives and two false positives. The receiver operating characteristic curves showed a sensitivity of 89.5% and a specificity of 81.3% when using a cutoff value of 2 mM 2HG (area under the curve 0.88).

It was found that 2HG MRS was easily implementable in a clinical context showing a high diagnostic accuracy. The 100% sensitivity and specificity described by Choi et al. [24] was, however, not achieved, which is most likely caused by our limited scan time. Sampling can be improved by adjusting the voxel size, by resampling several times, or by increasing the number of measurement repetitions per voxel, all of which extending the examination time. False positive and negative results could be explained by incorrect voxel positioning in three cases. The last, false negative case was an astrocytoma grade II with a very low proliferation rate, most likely producing only low concentration of 2HG.

This method will undoubtedly prove to be useful for preoperative tumour diagnosis, including differentiation from non-tumour diseases, and for disease monitoring, e.g. diagnosing tumour recurrence, treatment response, or pseudoprogression.

Study 4 and **study 5** represent optimisation studies. Translating new quantitative MRI techniques as in **study 1** - **3** helps to identify challenges, pitfalls, and sources of error that impede broader implementation or, in the worst case, lack of acceptance in the clinical community. **Study 4** and **study 5** focus on perfusion-weighted DCE MRI and compare curve-fitting algorithms in order to optimise parameter maps. The purpose of primarily **study 5** was to determine if the diagnostic reliability could be increased, thereby possibly accelerating the clinical translation of DCE MRI, a promising technique not only for brain tumours patients.

2.4 Bayesian modeling of Dynamic Contrast Enhanced MRI data in cerebral glioma patients improves the diagnostic quality of haemodynamic parameter maps

Anna Tietze, Anne Nielsen, Irene Klærke Mikkelsen, Mikkel Bo Hansen, Annette Obel, Leif Østergaard, Kim Mouridsen

PloS One 2018 Sep; 13(9): e0202906
https://doi.org/10.1371/journal.pone.0202906

Compared to DSC perfusion-weighted MRI DCE still has a relatively low acceptance in neuroimaging and neuroscience, although several advantages can be listed (for details see section 1.2.3). One reason are noisy parameter maps, especially when applying more complex vascular models. This complicates diagnosics considerably or, in the worst case, makes valid conclusions impossible.

A key step when using model-based approaches is to fit the model parameters to the measured DCE MRI data. This can be difficult in noisy or low-signal raw data or in more advanced models with many parameters. As described in more detail in **study 5** [56] standard curve-fitting meth-ods as the Levenberg-Marquardt (LM) approach [57] might be too simple for the rather complex fitting of DCE data to multi-parameter models. In this study, an alternative, probabilistic approach, the Bayesian method (BM), is proposed [58, 59]. The aim of this study was to compare both curve fitting methods with regard to the quality and diagnostic accuracy of parameter maps in clinical data.

The ETM and the 2CXM models, respectively, were fitted to the DCE data of 42 glioma patients using both methods (LM and BM). Imaging

was performed on a 3T Philips Achieva 3TX system (Philips Medical Systems, Best, Netherlands). Post-processing and the statistical analysis was done with Matlab (Mathworks, Natick, MA, USA) and R (Boston, MA, USA). The different parametric maps were presented randomly to two board-certified neuroradiologists who scored their diagnostic quality on a scale 1 to 4 with regard to tumour-to-background and tumour-to-vessel discrimination as well as overall impression. A logistic regression and an ordinal linear, mixed model were used to evaluate if there was a significant difference between image quality. A Wilcoxon signed-rank test was used to assess if the fitting algorithms had an impact on the diagnostic performance in discriminating high-grade from low-grade tumours. Here, the mean of K_{trans}, K_1, and V_p was measured in the contrast enhancing part of the tumour or in the T2FLAIR hyperintense region for non-enhancing tumours.

The image quality was especially improved in K_{trans}, K_1, and V_e maps, all of which describing the blood-brain-barrier, when using the BM curve fitting algorithm. The difference was significant for both readers ($p < 0.001$). Also, parameter maps generated with the 2CXM were superior regardless the applied fitting method. High- and low-grade tumours could only be differentiated reliably when using BM-based V_p and K_{trans}, the latter was unaffected by the underlying fitting algorithm. K_1 could not discriminate between tumour grades.

In conclusion, it was shown that BM improves the diagnostic performance of DCE parameter maps in brain tumours. 2CXM not only enables the separation of the blood-flow-related F_p from the permeability parameter K_1, but also improves image quality compared to the widely used ETM. This study has the potential to increase the acceptance of DCE in neuroimaging, thereby opening up for other application fields such as multiple sclerosis, cerebrovascular diseases, dementia etc. More commercial software solutions are needed to enable the clinical implementation.

2.5 Robust estimation of hemo-dynamic parameters in traditional DCE-MRI models

Mikkel, Bo Hansen, Anna Tietze, Søren Haack, Jesper Kallehauge, Irene Klærke Mikkelsen, Leif Østergaard, Kim Mouridsen

PloS One 2019 Jan; 14(1): e0209891
https://doi.org/10.1371/journal.pone.0209891

This study forms the theoretical basis for **study 4**. It addresses the central question of how to improve the diagnostic quality of DCE-based parameter maps by optimised curve fitting to the experimental data. Curve fitting describes the process of fitting a model, in our case the tracer-kinetic models ETM and 2CXM, to measured data. In DCE, LM has been found to be a useful fitting algorithm and is employed in most studies and commercial softwares. DCE data in the brain are, however, rather noisy and are challenged by relatively small signal changes during the contrast bolus passage, which makes fitting to the more complex 2CXM model especially difficult. Noisy and unreliable parameter maps are the result.

In this work, an alternative, statistical approach is suggested, the BM that is based on Bayesian inference. The basic concept of this method is that existing knowledge is used (termed *prior*) to deduce the probability of a certain, posterior distribution of data. In other words, parameter estimation is initialised by a prior value and covariance in each voxel and subsequently updated using a log-likelihood function. In this study, this updating procedure was done for a maximum of 32 iterations.

The performance of the algorithm was evaluated qualitatively using computer simulations in digital phantoms and patient data (6 patients with GBM and 5 patients with cervical cancer stage 3 IIB/2 IIIB) and com-pared to the well established LM curve fitting algorithm. Postprocessing was done using Matlab (Mathworks, Natick, MA, USA) and the Statistical Parametric Modeling toolbox version 12 (SPM 12).

It was found the the two fitting methods performed very similar in the digital phantoms, except for extreme situation with high intra-/extravascular flow and a large extravascular volume, where BM showed more consistent results. Interestingly, LM overestimated the 2CXM-based V_e considerably in situations where the transfer from the intra- to extravascular compartment was zero, which in non-CNS tissue is rare, but which is true in

healthy brain tissue with an intact blood-brain-barrier. In these regions, high-intensity voxels could be so numerous that anatomical details were no longer recognisable. These multiple spurious voxels were accordingly shown in the GBM patients outside the tumour, and BM-based V_e and to a minor degree F_p maps as well stood out by their clarity compared to their LM-based counterparts. It was concluded that BM should be preferred as fitting algorithm when using more complex compartmental models such as the four parameter 2CXM, which from the physiological viewpoint might be superior to the more simple three parameter ETM.

In **study 6** and **study 7** the focus was shifted to paediatric neuroimaging. **Study 6** exemplifies another very early step of clinical translation, this time of a novel postprocessing approach for an otherwise well established MRI technique. The aim of **study 6** was to develop a method to obtain quantitative information on dynamic processes, observed *in vivo* by CINE MRI and to test its clinical usefulness in children with brain malformations. This is only one application example and other areas of application are suggested.

2.6 Dynamic cerebellar herniation in Chiari patients during the cardiac cycle evaluated by dynamic magnetic resonance imaging

Mia Tietze, Andreas Schaumann, Ulrich-Wilhelm Thomale, Philip Hofmann, Anna Tietze

Neuroradiology 2019 Jul; 61(7): 825-832
https://doi.org/10.1007/s00234-019-02203-2

It is believed that apart from the direct brainstem and spinal cord compression the altered CSF flow patterns in Chiari patients lead to the development of symptoms. The hypothesis of this study was that compression and CSF outflow obstruction can be intermittent, as the herniation of the cerebellar tissue can be pulsatile during the cardiac cycle. Dynamic herniation can be assessed on CINE MRI sequences that generate time resolved image loops. Here, a quantitative method to measure movement during the CINE loop was developed and tested. It was compared to simple visual inspections that are usually done in the clinical context. In addition, the degree of herniation on dynamic and static images was com-pared, and it was assessed if herniation correlates with the development of ventriculomegaly and/or syringohydromyelia.

Twenty-seven children (mean age 8.45 $\pm$ 5.32 years) with CM2 (4 patients), CM1 (10 patients), craniosynostoses (10 patients), headache (1 patient), syncope (1 patient), or a lipomeningocele (1 patient) were retrospectively included. CINE sequences as well as conventional sequences including MPRAGE were acquired on a 3T MRI system (Siemens Magnetom Skyra, Erlangen, Germany). The visual inspection of the static, conventional images and the semi-quantitative assessment of the CINE loop was done using the open software HOROS (accessed 01/03/2021:

Horosproject.org; Nimble Co LLC d/b/a Purview, Annapolis, MD, USA). A quantitative method (voxel intensity distribution method (VIDM)) to measure dynamic herniation objectively was developed in Igor Pro (WaveMetrics, Lake Oswego, OR 97035, USA).

VIDM determines the interface between the hypointense cerebellar tissue and the hyperintense CSF by identifying the maximum intensity difference in the full CINE loop. The extent of movement can then be measured by following the maximum intensity difference over time. To avoid an uncertainty of $\pm$ 1 voxel, thereby accounting for partial volume effects, a Gauss-curve was fitted to the function. Transferring the CINE voxel size (in our protocol $1\times1\times4$ mm^3, where 4 mm is the slice thickness) to this approach, the herniation could then be reported in mm. True movement was defined as $\geqslant$ 3 standard deviations of the difference between the cerebellar tissue being in the most cranial and caudal position.

For the visual inspection, the distance between the cerebellar tissue in the most cranial and caudal position was measured on the imaging viewer. Ventriculomegaly was quantified using the frontal-occipito-horn-ratio [60] and syringohydromyelia was defined as a central canal widening of $>$ 2 mm.

In significantly more ($>$ 50%) cases craniocaudal movement was detected by VIDM than by visual inspection alone ($p = 0.002$). There was no correlation between the herniation and ventriculomegaly or syringohydromyelia. In most cases, the herniation appeared greater on conventional sequences than on CINE.

Even though we did not find any correlation between the dynamic herniation and the clinical outcome parameters, the detection of even small movements can be relevant in Chiari patients, e.g. to monitor the success of craniocervical decompression or to investigate the consequences of head positions or Valsalva manoeuvres. The described quantitative and automatic method allows, moreover, the confirmation of subtle movements of for example membranes, adhesions, third ventriculostomies, cyst walls etc. that might be difficult to detect on static images. VIDM can easily be transferred to every imaging field that investigates dynamic processes.

Study 7 is both a validation and a reproducibility study. T1 mapping based on the MP2RAGE sequence has been described in different neuroradiological contexts before. For **study 7**, the sequence parameters were modified in order to accelerate the acquisition, which is important when examining young and potentially uncooperative children. T1 relaxation maps were retrospectively generated from MRI data of a large cohort of infants and young children to quantify normal myelination. The aim was to draw attention to this powerful mapping technique using a fast and widely available diagnostic sequence and to provide a publicly available database of age dependent T1 values that can be used for comparison in diagnostics and research.

2.7 Assessment of myelination in infants and young children by T1 relaxation time measurements using the Magnetization Prepared 2 Rapid Acquisition Gradient Echoes sequence

Fabienne M. Kühne, Wolf-Julian Neumann, Philip Hofmann, José Marques, Angela M. Kaindl, Anna Tietze

Ped. Radiol. 2021 Oct; 51(11): 2058-2068
https://doi.org/10.1007/s00247-021-05109-5

T1 mapping, i.e. the voxel-wise quantification of T1 values, is a valuable technique to quantify myelin maturation. A recently described method uses the MP2RAGE sequence that provides T1 mapping data and has at the same time a high diagnostic value due to its excellent contrast and resolution [46]. This sequence has been part of many paediatric imaging protocols at the Institute of Neuroradiology, Charité - Universitätsmedizin Berlin, since 2017. The aim of this study was to provide T1 data for comparison in the age group up to 24 months, where data on a larger scale so far are missing. Children up to six years were included in order to be able to compare with the literature. Due to ethical reasons MRI data in entirely healthy children are difficult to acquire. Children with a low risk of cerebral disease imaged between July 2017 and April 2020 were identified. This was accomplished by including children with normal MRI findings both prior and after inclusion and negative clinical findings. These data were compared to those of children with different brain pathologies.

MRI data of 94 MRI-negative children (60 males; mean age 34.4 months $\pm$ a standard deviation of 20.9 months) and 36 children (24 males; 39.7 $\pm$ 22.1 months) with different pathologies were retrospectively analysed. Imaging was done on a 3T Siemens system (Skyra Magnetom, Siemens, Erlangen, Germany). MatLab (Mathworks, Natick, MA, USA) and ITK-SNAP [61] were used for post-processing and analysing the data. Statistics was done with Igor Pro (WaveMetrics, Lake Oswego, OR 97035, USA). Mean T1 values were extracted from 17 white and grey matter regions in all 130 datasets. Relaxivity (R1=1/T1) was plotted as a function of age and exponential functions were fitted to the data. Finally, the MP2RAGE data were compared qualitatively to standard T1- and T2-weighted images with regard to contrast and myelination patterns.

R1 plots, the myelination rate, and the myelination state at birth were specified for the 17 regions. As expected, R1 was highest at birth in well myelinated structures (e.g. the posterior limb of the internal capsule). Myelination proceeded fastest in the corpus callosum and was particularly slow in the deep grey matter. Most children in the pathology group displayed normal T1 values, i.e. their values lied within the uncertainties of those by the MRI-negative individuals. The qualitative evaluation of the MP2RAGE data showed that signal intensities change in the same spatial order, but over a considerably longer time period (almost up to the age of 6 years) compared to conventional T1- and T2-weighted data (where signal changes are only observed up to the age of 2 years).

This works provides T1 data for an age group that is underrepresented in the literature so far, although the major part of myelination takes place during this period. Only very few children of our pathology group had, however, abnormal T1 values in the brain regions we evaluated. The MP2RAGE allows to visualise myelin maturation up to the age of 6 years, whereas T1- and T2-weighted images lead us to believe that myelination is complete at the age of 2 years. That myelination continues well into adulthood is known from studies using other advanced MRI methods [62]. It needs to be elucidated what microstructural changes cause the observed MP2RAGE signal alterations. We believe that this T1 mapping technique is easily implementable, could enable an automatic, objective myelination assessment, and at the same time provide high quality diagnostic imaging data.

Chapter 3

Discussion

The aim of this work was to translate qMRI techniques from the research environment into the clinical context, to explore their feasibility and limitations and to apply them in different pathologies. As a first step, new method are usually developed in phantoms and in preclinical, mostly animal models before they are validated in healthy volunteers, subsequently moving on to the clinical setting, where they have to be tested for repeatability and reproducibility [63]. This way can be long and winding and not every technique is translatable to the clinics or might not even be designed for that.

Five methods in different stages of clinical translation were presented with all of them having in common to derive quantitative information that can expand the common qualitative assessment of MRI data by additional metabolic, functional, or microstructural information. The undisputed advantage of qMRI are furthermore robust and objective measures that allow for higher intra- and interrater reproducibility, more valid longitudinal assessment, and finally diagnostic confidence.

3.1 Stages of clinical translation

The implementation starts with the development of either new MRI acquisition techniques or postprocessing procedures. **Study 6** exemplifies this early step by presenting a novel postprocessing approach to measure subtle movements of anatomic structures on dynamic CINE MRI [64]. This study was primarily methodical and applied in a small cohort of children

with brain malformations, where intermittent brainstem compression due to CSF pulsatility can lead to symptoms.

The next step of translation is the application in larger patient cohorts or different pathologies to explore the techniques' usefulness in various contexts. **Study 1** and **study 2** represent this stage [65, 66]. Here, the recently in animal models, healthy subjects, and small patient groups developed ph-weighted APT imaging technique was for the first time applied in acute stroke patients and a patient with a prolonged migraine aura. The APT sequence had to be adapted to the acute setting of stroke patients who still were in the therapeutic window, where time is important. Especially **study 1** helped to define technical limitation, an essential step on the way from "bench to bedside".

Also in **study 3** and **study 7**, intermediate steps of translation are investigated [67]. In **Study 3**, the repeatability of 2HG MRS in glioma patients to detect the IDH mutational status was tested. 2HG MRS is a further development of the well established, general MRS that for this study was expanded by a quantitative approach. Although applied in glioma patients before, none of these studies were made in a clinical setting, where lengthy measurements are not an option. The diagnostic accuracy was decreased in comparison, albeit little, and ways to improve it could be pointed out.

Study 7 represents a further validation study and thereby an important step of clinical translation. This time, the MRI sequence applied had to be accelerated considerably, as children, often uncooperative, were examined. In spite of that, the T1 mapping method described here provided robust T1 values in a large cohort of infants and young children.

Study 4 and **study 5** consider a different aspect of clinical translation [58, 68]; the perfusion-weighted MRI sequence described here is a relatively well established technique, but reproducibility issues of quantitative parameters are a major concern impeding proper clinical implementation. Sources of variability are diverse, i.e. hardware, operator, or analysis dependent. In these studies, analysis steps, in particular curve-fitting methods, are compared in phantoms and patient data and optimisation procedures suggested.

3.2 The clinical significance of quantitative MRI biomarkers in patients with ischaemic stroke, gliomas, Chiari malformations, and during normal brain maturation

3.2.1 MRI biomarker for prediction of tissue at risk in ischaemic stroke patients

The therapy for acute ischaemic stroke patients has been revolutionised since the first trial investigating the effect of intravenous thrombolysis in 1995 [69] and several subsequent studies have confirmed the improved, clinical outcome of stroke patients thanks to this treatment [70–72]. Ten years later, the first results of safety and efficacy of mechanical thrombectomy were published [73] and after a fast-paced development of new thrombectomy devices, mechanical revascularisation is today an integral part of treatment [74–76].

Well defined clinical and imaging criteria to select for appropriate therapy are essential for the management of ischaemic stroke patients in order to achieve the best outcome with as few complications as possible [76–78]. Treatment selection, i.e. thrombolysis, mechanical thrombectomy, or none of these, is the result of patient- (i.e. symptoms, contraindications) and imaging-related (infarction, tissue at risk, contraindications) factors. The general principle today to proceed with recanalisation therapies is the time-based approach to balance the predicament of treatment success and complications. Guidelines specify the therapeutic window (currently max. 4.5 - 6 hours after onset of symptoms for intravenous thrombolysis, approx. max. 6 hours for thrombectomy), well aware that this therapeutic window may vary between patients, probably owing to differences in the efficiency of collateral supply.

The ischaemic injury is a continuum of hypoperfusion and usually divided in different categories; the infarction core, i.e. the unsalvageable tissue, is characterised by symptomatic hypoperfusion, ischaemia is symptomatic, hypoperfused, but salvageable tissue, and asymptomatic oligaemia does not require recanalisation. It is important to remember that these definitions are based on physiological/metabolical criteria and not on imaging [79]. Current MRI and CT protocols do not differentiate sufficiently between different degrees of hypoperfusion, which is a limitation for the best

treatment.

The described difficulties in defining oligaemic tissue and to distinguish it from symptomatic ischaemia and the infarct core was the motivation for **study 1**. Only a small patient cohort was included in this primarily proof-of-principal-study and statistical significant results could not be expected, but tissue acidosis as a result of hypoperfusion and anaerobic glycolysis could be detected and indicated correct prediction of final infarct size.

The interpretation of APT effects in ischaemic tissue is, however, not straightforward. Signal changes are not evoked by acidosis alone, but by the concentration of amides that might be increased due to post-ischaemic inflammation and of lactate that can be washed-out in partially reperfused tissue. Both effects are, however, expected to be small in the hyperacute stroke patients of this study. Moreover, overlying, subvoxel T1 and T2 effects as well as pseudo-normalisation through presumably buffering processes in the infarct core can influence the APT effect [80] that have to be taken in account when interpreting results.

3.2.2 MRI biomarker for brain tumour classification, grading, and molecular subtyping

Imaging-based brain tumour classification and grading has a long tradition in neuroradiology. A multitude of studies have been published since 1990 including perfusion-weighted [10, 28, 81], diffusion-weighted [9, 82], or MRS imaging [83, 84]. The rationale behind imaging strategies that go beyond the simple qualitative evaluation of conventional MRI data is the detection of metabolic changes that are a consequence of increased cell proliferation, neo-angiogenesis, tissue hypoxia etc. The aim is to accomplish the presurgical assessment of tumour type, i.e. primary brain tumour versus brain metastases, tumour grading and subtyping, the visualisation of particularly active tumour regions for targeted biopsies, and to diagnose treatment response or treatment related tissue damage.

Study 3 describes how to quantify certain brain metabolites *in vivo* by means of MRS [67]. The study is a reliability and reproducibility study of 2HG MRS to diagnose the IDH mutational status in glioma patients. IDH mutations are a key characteristics of cerebral gliomas, where IDH wildtype status is associated with considerably worse outcome [85]. This method had been described and clinically tested before, but that was still

done in a research environment, where repeated and lengthy acquisitions were possible [24]. We implemented it on a busy, clinical department, and were thus only able to do a single measurement per patient, using a time-optimised protocol. We still achieved a very high diagnostic accuracy (correct prediction in 88.6% of our patients; 89.5% sensitivity and 81.3% specificity). Although this is lower than previously reported [24], it is still a very good compromise between examination times and results. We furthermore propose several aspects to optimise data acquisition, very likely to increase accuracy even more, e.g. increasing the number of averages per voxel, resampling in different tumour regions, or decreasing the voxel size.

This qMRI techniques fascinates with its easy implementation, as a common MRS sequence is used and with fast postprocessing allowing the straightforward adoption in clinical protocols. In addition, the quantification method enables intra- and interindividual as well as longitudinal comparison [21]. One might argue that the determination of the IDH mutational status is not absolutely necessary, because in most cases tumour tissue would be available *ex vivo* after biopsy or resection, but it was found that 2HG MRS was especially useful for the differentiation between tumour and non-tumour, e.g. in the case of tumefactive multiple sclerosis, where surgery is not indicated [67]. The work was published only two years after the publication of the revised 2016 WHO classification for brain tumours that highlight the immense impact of diagnosing the IDH mutational status in glioma patients.

While **study 3** describes an imaging biomarker for subtyping of gliomas, **study 4** and **study 5** concerns perfusion related biomarkers, in particular DCE-based parametric maps. These are traditional metrics to evaluate neo-angiogenesis and the blood-brain-barrier, both important characteristics of high-grade gliomas. The studies represent optimisation studies and suggest a curve-fitting method based on Bayesian inference for DCE data to avoid miscalculation on a voxelwise basis. The improved quality of the resultant maps was especially evident for parameters related to the blood-brain-barrier, i.e. K_{trans}, K_1, and V_e. These metrics are valuable for tumour grading, foremost relevant for the evaluation of anti-angiogenic treatment, where the microvascular permeability is altered [86]. The advantage of the BM was most noticeable, when using the more complex, four parameter 2CXM model that is physiologically more meaningful, but rarely implemented in postprocessing software. It is speculated that the

reason lies in the standard curve-fitting algorihm LM that copes with the more elaborate models only with difficulties.

The difference between the two approaches was most pronounced in healthy white and grey matter. Spurious voxels on the LM-based parameter maps could be so numerous that small satellite tumours or perifocal changes were no longer visible. This is not only a problem for quantitative approaches, but also prevent the implementation of DCE MRI as a qualitative imaging tool.

It is obvious that a sound quality of the parametric maps is an essential prerequisite for a broad acceptance in the clinical community. In these studies, the high demands on hardware and the lengthy BM-based calculations were found to be a limiting factor for the use in a clinical context. Approaches to speed the processes up are, however, suggested and to date, commercial software solutions for DCE imaging based on the Bayes' theorem have become available (accessed 01/03/2021: `https://www.cercare-medical.com`, `https://www.olea-medical.com/en`).

3.2.3 In vivo quantification of dynamic cerebellar herniation in Chiari pateints

In **study 6**, time-resolved loops of MR images were acquired in children with Chiari malformations and craniosynostoses, both malformations, where cerebellar tissue herniates through the foramen magnum [64]. In this study, a measurement approach was developed to capture subtle movements with sub-voxel precision. Achieving such precision is essential for a meaningful interpretation of time-resolved MRI data. After all, the voxel size is usually chosen to be rather large to achieve acceptable signal-to-noise ratios for data collected in small time steps, and many important dynamical changes thus take place on a sub-voxel length scale.

To the best of our knowledge, our work is the first quantitative analysis of this kind. Real-time or CINE MRI originates from cardiovascular imaging, but covers today also joint dynamics, bowel, and foetal imaging as well as the observation of swallowing, tongue, and vocal cord movement. These images are usually assessed qualitatively to observe function. The analysis program described in this study provides a new tool to quantify even small movements that is not only valuable for Chiari patients, but also membranes and ventricular or cyst walls in the CNS. Outside the brain,

a multitude of applications is conceivable, where vocal cord movement, dynamics of the cardiac valves, cardiac wall motion abnormalities, foetal motor behaviour are only examples. The collection and analysis of CINE MRI data can be expected to gain importance with technical progress in data collection and processing. The quantitative analysis of CINE MRI data will undoubtedly be an integral part of such a development.

3.2.4 Longitudinal T1 relaxation time measurement as a quantitative imaging biomarker for brain myelination in children

Myelin consists of extensions formed by oligodendrocytes that wrap around neuronal axons and is indispensable for proper and rapid nerve conduction in the CNS. Myelin starts to develop during the late prenatal weeks and continues to form and mature during childhood and early adulthood. Myelination is usually assessed qualitatively in the clinical setting, i.e. the spatial and temporal evolution of signal changes is observed on T1- and T2-weighted images that is thought to be caused by the interaction of water protons with macromolecules (cholesterol, galactocerebosides, and proteins) in the developing myelin.

The assessment of myelination appropriate for age requires experience and subtle alterations may escape even the practiced radiologist. Quantitative approaches are obvious here and different methods to do so have been applied previously [87–91]. T1 mapping is one of several quantification methods and is a well established technique. Several mapping methods have been described [45], but substantial data of normally developed and healthy children under the age of 24 months, where the main part of myelination is taking part are scarce.

In **study 7**, T1 relaxation time measurements were performed in children without any pathology detected on clinical MRI. A large normative database of 94 MRI-negative infants and young children could be retrospectively created, because a recently described sequence, the MP2RAGE, is part of many diagnostic protocols for qualitative assessment, but can also be used for T1 mapping.

The expected longitudinal and spatial changes of T1 values described in two small, previous studies [47, 50] could be reproduced and myelination rates in different grey and white matter regions were determined. Most

importantly, this study provides normative data in a very young age group that are publicly available for diagnostics and research. It is suggested that T1 maps are calculated directly on the MRI scanner console and are available to diagnostics comparable to diffusion-weighted metrics. Moreover, parametric maps highlighting discrepancies between a patient and normal population data would make the diagnostic workflow faster and saver.

3.3 Limitations of the presented studies

The main limitation of **study 1** - **4** and **study 6** are the inclusion of relatively small patient cohorts. This applies foremost for **study 1** and **study 2** that are performed in a very early translational stage of APT imaging. Technical and ethical reasons precluded the inclusion of larger patient numbers in **study 1**, where acute stroke patients in the therapeutic window were imaged. MRI-compatible syringes would enable intravenous thrombolysis during image acquisition and would open up for larger studies without delaying timely treatment. **Study 2** was merely a descriptive report and a proof of principle. It was intended to shed some light on the pathophysiology of migraine aura in FHM patients and to draw attention to APT and perfusion-weighted imaging as a tool to investigate CSD. It is unlikely that the inclusion of larger patient cohorts in **study 3**, **4**, and **6** would have altered the results fundamentally, although this remains a matter of speculation.

A further limitation of **study 1** and **6** is the heterogeneity of included patients. In **study 1** (APT imaging in acute stroke), treatment varied across the patient population influencing clinical and imaging outcome considerably, why statistically relevant conclusion could not be drawn. Also the quantification of cerebellar herniation in **study 6** was tested in a rather inhomogeneous population consisting of CM1, CM2, and craniosynostosis patients. Nevertheless, the focus of the last study was to introduce a novel quantification method that can be applied in other fields in the future.

In **study 4**, only two neuroradiologists rated the quality DCE-based perfusion maps. Although both were experienced in general neuroradiology and tumour imaging, the amount of expert knowledge in DCE MRI differed between them. Especially the evaluation of low-grade gliomas on DCE parameter maps requires some experience, because they can be difficult

to discern. This might have influenced the results in the end.

The CINE MRI sequence that was configured for **study 6** was a compromise between imaging time and resolution. As imaging voxels were rather large, partial volume effects are an issue. Decreasing slice thickness would have increased the acquisition time inevitably, which was not an option, as many of the included patients were children not always willing or able to lie still for longer times. It was speculated that especially small structures, e.g. the Liliequist membrane that can be of importance in patients with hydrocephalus, would not be discernible with the applied imaging parameters. This appears, however, not to be the case as is found in an ongoing study in hydrocephalic children (not included in the present work). The main limitation of **study 6** is the lack of clinical correlation, which has to be addressed in the future.

The need to reduce acquisition times led also to modifications of the MP2RAGE sequence used for T1 mapping in **study 7**. Acceleration reduces inevitably the signal-to-noise ratio, which in turn can cause less precise measurements. By using a high quality 64-channel head coil this limitation was partly met. The main drawback of this study was that this normative database does not include entirely healthy children. Ethical reasons preclude to sedate or anaesthetise subjects and children in particular to acquire MRI data for research purposes only. Therefore "MRI-negative" infants and children were part of this retrospective study, mostly examined for suspected, but not stated pathologies (malformations, traumatic brain injury, infections) as well as for uncomplicated headaches. This was affirmed by negative clinical findings and normal previous and follow-up MRI if performed in the subject.

3.4 Aspects of quantitative MRI that may be limiting for clinical translation and need to be considered

All qMRI studies presented here have in common that additional, often commercial programming software have to be at hand. This has not only an economic impact, but often requires expert knowledge that might not be available outside academic hospitals. The multidisciplinary approach that has enabled the presented studies is the undisputed strength and prerequisite for the clinical translation of complex qMRI techniques, but can

also be regarded as a drawback. Full clinical implementation and further development require therefore easily accessible and automatic workflows that currently are not always available for the methods described. In these preliminary stages, postprocessing can be cumbersome and make high demands on computational power and postprocessing times. This is often not compatible with clinical demands, but the rapid technical development of both hard- and software allows these limitations to be minimised in the future.

A fundamental problem translating research techniques to clinical MRI systems can be their lower field strengths (usually 1.5 or 3T compared to 9.4T or even 21T in ultra high field research systems), which results in lower signal-to-noise and contrast-to-noise ratios. Also, safety limitations have to be considered in the clinics, and a not negligible number of patients have medical devices implanted that are not compatible with high energy radiofrequency pulses. Novel sequences are often not available on commercial MRI systems and many research techniques require a manipulation of the scanner software that is usually not possible without permission by the vendor. Most significant are, however, time constraints in the clinical settings. Particularly patients in a poor clinical state, with hyperacute conditions, or young children who need to be anaesthetised for the examination must not or are not able to remain in the scanner any longer than necessary. Moreover, the efficient use of health care resources is mandatory, balancing reliable, high-quality imaging, economic viability, and clinical pragmatism.

While translating novel MRI techniques from the research to the clinical context has been the primary focus of this work, the particular emphasis of all presented studies lies on new approaches that make use of the quantitative information contained in the data, thus going beyond a simple qualitative analysis of image material. Quantification has the undisputed advantage of providing reader-independent, consistent MRI data across imaging platforms and time. qMRI is therefore of key importance when imaging endpoints in clinical trials are needed, and quantitative data are often easier to process from a statistical point of view.

Repeatability and reproducibility studies of qMRI methods are of utmost importance before they are implemented clinically on a larger scale. Without careful parameter adjustment results can vary across MRI systems of different manufactures, with different softwares, and different field

strengths. While some sources of compromised reproducibility and precision can be avoided, e.g. by consistent patient positioning in the scanner, well defined regions of interest on the parameter maps, or appropriate parameter settings, other interfering issues cannot be influenced. That includes MRI system dependent factors, such as frequency and phase drift or non-uniform B_0/B_1 field as well as room temperature and humidity instability or software upgrades. Different postprocessing approaches can introduce further bias and should be avoided in multi-centre studies. An extensive review addressing the variability of the most important qMRI techniques is given in [92].

Several repeatability and reproducibility studies have been conducted for different organs, e.g. in the field of T1 and T2 mapping techniques [93–95], fingerprinting MRI [96], diffusion tractography [97], or DCE MRI [34, 98]. Naturally, results vary significantly depending on the technique examined. The variability ranges from 69% within-subject coefficient of variation for K_{trans} in DCE of uterine fibroids [34] to 0.4% inter-site MP2RAGE-based T1 measurements at 7 Tesla in cerebral grey matter [99]. The alarming results for the DCE study are certainly caused by many factors, e.g. the underlying model, T1 mapping technique, choice of arterial input function, and insufficient protocol harmonisation, but may also be induced by noisy parameter maps, a fact, that was investigated in the present work [58, 68].

3.5 Outlook

The most important future importance of qMRI lies undoubtedly in its role as a prerequisite for data digestion by machine learning approaches. While still in its infancy and not yet common in the clinical context, machine learning has already been successfully implemented for tasks such as simple image recognition and automated tissue segmentation, including volumetric assessment of brain tumours, as well as the prediction of pathology and patient outcome [100–102]. Supervised machine learning techniques require huge amounts of training data for learning specific tasks and such data sets are necessarily collected on different types of scanners, using different data acquisition protocols. The use of quantitative tools such as bias-field correction and different approaches to data normalisation are mandatory for the further data treatment by, e.g. convolutional neural networks (see [103] and references therein). Future developments

will include the evaluation of multimodal data that also need to be provided on a quantitative basis for a meaningful treatment. Machine learning methods will undoubtedly revolutionise clinical practice and the list of applications is growing daily. Providing reliable qMRI data is pivotal to this development.

Specifically, of the methods described in this thesis the quantitative approach VIDM to measure dynamic processes on CINE MRI is currently employed in a study of children with hydrocephalus. Under the assumption of altered pressure gradients between the third ventricle and the prepontine cistern in patients with CNS underdrainage, the extent of movement of the third ventricular floor is measured. A further study assessing movement of the spinal cord conus prior and after de-tethering surgery is planned. Relaxometry data in healthy children and children with different cerebral diseases is currently initiated using a quantitative multiparametric approach that is optimised for the clinical routine due to short acquisition times [104]. And last but not least, automated algorithms for tissue segmentation based on convolutional neural networks are tested and optimised for adult and paediatric brain tumour patients in order to have a better monitoring tool available for treatment response assessment.

Chapter 4

Summary

The overall objective of the present work is the translation of advanced qMRI techniques from the research environment into the field of clinical neuroimaging. In this context, qMRI is defined as the application of absolute quantitative measures that are extracted from *in vivo* MRI data. These can be used to describe biophysical characteristics and processes and thereby enhance the diagnostic power of qualitative, "weighted" imaging that is primarily used in the clinical setting. The feasibility, usefulness, and limitations of five qMRI techniques were investigated in different CNS pathologies (brain tumours, ischaemic stroke, migraine, brain/skull malformations) and in the description of normal brain maturation in infants and young children. The translation of new imaging methods from "bench to bedside" involves several steps, and the presented studies are located at different stages in this process.

Studies 1 and **2** are examples of a relatively early stage. At the time of publication, pH-weighted APT imaging had been tested preclinically and in smaller cohorts of patients, but not in acute stroke, where anaerobic glycolysis and tissue acidosis is highly prevalent. In **study 1**, it was postulated that APT imaging could be a novel approach to demonstrate oligaemia in hyperacute stroke, allowing a more detailed description of tissue at risk. For acceleration purposes, sequence parameters were optimised by using computer simulations and subsequently validated in healthy subjects. Ten acute stroke patients were included ($7 < 4$ hours, $3 < 24$ hours after symptom onset). As expected, the APT effect was significantly decreased in ischaemic regions compared to normal white matter (p=0.03) and APT values tended to be lower in the final infarct volume

(p=0.10). In **study 2**, APT imaging was moved to a different pathology, also characterised by hypoperfusion, tissue hypoxia, and anaerobic glycolysis. Here, the metabolic changes during the migraine aura of a patient with FHM were investigated for the first time using APT imaging. The patient developed clear tissue acidosis and blood flow disturbances in the absence of ischaemia in the affected cerebral hemisphere, possibly caused by CSD, i.e. the state of neuronal inhibition that is supposed to be the pathophysiological basis of migraine aura. The studies were not designed to provide a statistical conclusion, but to identify technical strengths and weaknesses of this imaging technique.

Study 6 also represents an early phase of clinical translation. Here, a new postprocessing approach was developed to achieve absolute metrics for the measurement of dynamic processes on CINE MRI, a time-resolved method to visualise moving structures *in vivo*, e.g. in cardiac, bowel, or foetal imaging. Usually movement is evaluated qualitatively and to date objective quantitative approaches are missing. In this study, a measuring method (voxel intensity distribution method, VIDM) for subtle movements was developed and applied in 27 children with Chiari and other brain/skull malformations, where cerebellar tissue herniates dynamically through the foramen magnum following CSF pulsatility. The degree of movement was compared using VIDM and visually derived, clinically accepted linear measurements on CINE sequences. In 85% of the patients, VIDM showed significantly more cerebellar displacement (p=0.002) compared to simple visual assessments, although this did not correlate with the clinical outcome parameters (hydrocephalus or syringomyelia; Pearson's correlation coefficient -0.28; p=0.16). It is suggested that VIDM might be a valuable tool to detect and measure subtle dynamic processes in the CNS, but extracranial applications are also very likely.

Study 3 and **7** represent validation studies of methods that have been presented in clinical data before. In **study 3**, 2HG MRS was used in 35 patients suspected for cerebral gliomas to determine the IDH mutational status that today is an integral part of the WHO brain tumour classification system. For this study, a dedicated MRS sequence was used and the routine imaging protocol was extended by only 6 min. The sensitivity/specificity for determining the IDH mutational status was 89.5% and 81.3%, respectively. It could be concluded that 2HG MRS is an easily applicable supplement to standard imaging protocols that allows presurgical diagnostics and opens up for more detailed assessment during

treatment.

In **study 7**, T1 maps were generated from clinical MRI data using the MP2RAGE sequence, a technique extensively applied in neuroscience, but little in the clinical setting. The technical parameters were adapted to find a balance between short acquisition times, high signal-to-noise, and reliable T1 values to quantify myelin maturation in 94 children up to the age of 6 years. The assessment of adequate myelination is a central part of paediatric imaging diagnostics, but is to date done by evaluating images qualitatively. The aim was to validate the MP2RAGE-based T1 mapping technique for the assessment of normal myelination, and data were compared to those of children with various CNS pathologies. Additionally, the diagnostic power of the MP2RAGE was pointed out for the qualitative assessment of regular myelination and brain pathologies.

The purpose of **study 4** and **5** was to improve the diagnostic confidence of perfusion-weighted DCE maps. DCE is a well-established technique outside the CNS, but is used less in neuroimaging due to a number of technical issues. Here, postprocessing was addressed with the aim to reduce noise in the resultant parameter maps. Two curve-fitting methods, the Levenberg-Marquardt (LM) algorithm and a Baysian method (BM), were compared in digital phantoms and in 42 glioma patients applying two compartmental models (extended Toft's, ETM, and 2-compartment-exchange model, 2CXM). The image quality was assessed with regard to tumour discrimination and overall impression of the images. Moreover, the diagnostic performance to differentiate high-grade from low-grade gliomas was investigated. The image quality of parameter maps generated by BM was significantly improved compared to LM ($p<0.001$), and the 2CXM-based maps were higher rated, regardless of the fitting method. The diagnostic performance to differentiate tumour grades was excellent for K_{trans} and V_p ($p<0.001$). This was not affected by the fitting method for the leakage parameter K_{trans}, whereas V_p was improved when using BM. These studies suggest that using BM to derive perfusion parameters from DCE data are superior to LM, hopefully leading to higher diagnostic confidence and acceptance in the clinical community.

Clinical imaging diagnostics benefits without doubt from the integration of quantitative information gained by qMRI, thereby increasing reproducibility and reliability and enabling the objective comparison to normative and patient databases. Each step of the clinical translation process is essen-

tial to show opportunities, identify areas of optimisation, and to reveal challenges and limitations. After further development APT imaging is today available on standard MRI platforms, and BM-based curve fitting of perfusion data has been implemented in postprocessing software programmes. T1 maps of normal myelination in children are made publicly available and may be a first step towards an automated tool to detect myelination disorders more efficiently.

Chapter 5

Publications related to this thesis

Study 1
Tietze A, Blicher JU, Mikkelsen IK, Østergaard L, Stroher MK, Smith SA, Donahue MJ. Assessment of ischaemic penumbra in patients with hyperacute stroke using amide proton transfer (APT) chemical exchange saturation transfer (CEST) MRI. NMR in Biomedicine. 2014 Feb; 27(2): 163-174.

Study 2
Blicher JU, Tietze A, Donahue MJ, Smith SA, Østergaard L. Perfusion and pH MRI in familial hemiplegic migraine with prolonged aura. Cephalalgia. 2016 Mar; 36(3): 279-283.

Study 3
Tietze A, Choi C, Mickey B, Maher EA, Ulhøi BP, Sangill R, Lassen-Ramshad Y, Lukacova S, Østergaard L, Oettingen G. Noninvasive assessment of isocitrate dehydrogenase mutation status in cerebral gliomas by magnetic resonance spectroscopy in a clinical setting. J Neurosurg. 2017 Feb; 128(2): 391-398.

Study 4
Tietze A, Nielsen A, Mikkelsen IK, Hansen MB, Obel A, Østergaard L, Mouridsen K. Bayesian modeling of Dynamic Contrast Enhanced MRI data in cerebral glioma patients improves the diagnostic quality of haemodynamic parameter maps. PloS One. 2018 Sep; 13(9): e0202906.

Study 5
Hansen MB, Tietze A, Haack S, Kallehauge J, Mikkelsen IK, Østergaard L, Mouridsen K. Robust estimation of hemo-dynamic parameters in traditional DCE-MRI models. PloS One 2019 Jan; 14(1): e0209891.

Study 6
Tietze M, Schaumann A, Thomale UW, Hofmann P, Tietze A. Dynamic cerebellar herniation in Chiari patients during the cardiac cycle evaluated by dynamic magnetic resonance imaging. Neuroradiology 2019 Jul; 61(7): 825-832.

Study 7
Kühne FM, Neumann WJ, Hofmann P, Marques J, Kaindl AM, Tietze A. Assessment of myelination in infants and young children by T1 relaxation time measurements using the Magnetization Prepared 2 Rapid Acquisition Gradient Echoes sequence. Ped. Radiol. 2021 Oct; 51(11): 2058-2068.

Chapter 6

Bibliography

[1] Tournier JD, Calamante F, Gadian DG, Connelly A. Direct estimation of the fiber orientation density function from diffusion-weighted MRI data using spherical deconvolution. Neuroimage. 2004 Nov;23(3):1176–85.

[2] Hui ES, Cheung MM, Qi L, Wu EX. Towards better MR characterization of neural tissues using directional diffusion kurtosis analysis. Neuroimage. 2008 Aug;42(1):122–34.

[3] Hernandez-Garcia L, Lahiri A, Schollenberger J. Recent progress in ASL. NeuroImage. 2019 Feb;187:3–16.

[4] Hua J, Liu P, Kim T, Donahue M, Rane S, Chen JJ, et al. MRI techniques to measure arterial and venous cerebral blood volume. NeuroImage. 2019 Feb;187:17–31.

[5] Germuska M, Wise RG. Calibrated fMRI for mapping absolute CMRO2: Practicalities and prospects. NeuroImage. 2019 Feb;187:145–153.

[6] Liu P, De Vis JB, Lu H. Cerebrovascular reactivity (CVR) MRI with CO2 challenge: A technical review. NeuroImage. 2019 Feb;187:104–115.

[7] Jespersen SN, Østergaard L. The roles of cerebral blood flow, capillary transit time heterogeneity, and oxygen tension in brain oxygenation and metabolism. J Cereb Blood Flow Metab. 2012 Feb;32(2):264–77.

[8] Law M, Young R, Babb J, Rad M, Sasaki T, Zagzag D, et al. Comparing perfusion metrics obtained from a single compartment versus pharmacokinetic modeling methods using dynamic susceptibility contrast-enhanced perfusion MR imaging with glioma grade. AJNR Am J Neuroradiol. 2006 Oct;27(9):1975–82.

[9] Tietze A, Hansen MB, Ostergaard L, Jespersen SN, Sangill R, Lund TE, et al. Mean Diffusional Kurtosis in Patients with Glioma: Initial Results with a Fast Imaging Method in a Clinical Setting. AJNR Am J Neuroradiol. 2015 Aug;36(8):1472–8.

[10] Tietze A, Mouridsen K, Lassen-Ramshad Y, Ostergaard L. Perfusion MRI derived

indices of microvascular shunting and flow control correlate with tumor grade and outcome in patients with cerebral glioma. Plos One. 2015;10(4):e0123044.

[11] Schellinger PD, Bryan RN, Caplan LR, Detre JA, Edelman RR, Jaigobin C, et al. Evidence-based guideline: The role of diffusion and perfusion MRI for the diagnosis of acute ischemic stroke: Report of the Therapeutics and Technology Assessment Subcommittee of the American Academy of Neurology. Neurology. 2010 Jul;75(2):177–185.

[12] Saver JL. Time Is Brain—Quantified. Stroke. 2006 Jan;37(1):263–266.

[13] Gasparetto EL, Cabral RF, da Cruz LCH, Domingues RC. Diffusion Imaging in Brain Infections. Neuroimaging Clinics of North America. 2011 Feb;21(1):89–113.

[14] Ledig C, Schuh A, Guerrero R, Heckemann RA, Rueckert D. Structural brain imaging in Alzheimer's disease and mild cognitive impairment: biomarker analysis and shared morphometry database. Scientific Reports. 2018 Jul;8(1):11258.

[15] Zhou J, Heo HY, Knutsson L, van Zijl PCM, Jiang S. APT-weighted MRI: Techniques, current neuro applications, and challenging issues. Journal of Magnetic Resonance Imaging. 2019 Jan;50(2):347–364.

[16] Jiang S, Eberhart CG, Zhang Y, Heo HY, Wen Z, Blair L, et al. Amide proton transfer-weighted magnetic resonance image-guided stereotactic biopsy in patients with newly diagnosed gliomas. European Journal of Cancer. 2017 Sep;83:9–18.

[17] Zhou J, Payen JF, Wilson DA, Traystman RJ, van Zijl PCM. Using the amide proton signals of intracellular proteins and peptides to detect pH effects in MRI. Nature Medicine. 2003 Jul;9(8):1085–1090.

[18] Zhao X, Wen Z, Huang F, Lu S, Wang X, Hu S, et al. Saturation power dependence of amide proton transfer image contrasts in human brain tumors and strokes at 3 T. Magnetic Resonance in Medicine. 2011 Mar;66(4):1033–1041.

[19] Alger JR. Quantitative Proton Magnetic Resonance Spectroscopy and Spectroscopic Imaging of the Brain. Topics in Magnetic Resonance Imaging. 2010 Apr;21(2):115–128.

[20] Tong Z, Yamaki T, Harada K, Houkin K. In vivo quantification of the metabolites in normal brain and brain tumors by proton MR spectroscopy using water as an internal standard. Magnetic Resonance Imaging. 2004 Sep;22(7):1017–1024.

[21] Choi C, Raisanen JM, Ganji SK, Zhang S, McNeil SS, An Z, et al. Prospective Longitudinal Analysis of 2-Hydroxyglutarate Magnetic Resonance Spectroscopy Identifies Broad Clinical Utility for the Management of Patients With IDH-Mutant Glioma. Journal of Clinical Oncology. 2016 Nov;34(33):4030–4039.

[22] Louis DN, Perry A, Reifenberger G, von Deimling A, Figarella-Branger D, Cavenee WK, et al. The 2016 World Health Organization Classification of Tumors of the Central Nervous System: a summary. Acta Neuropathol. 2016 Jun;131(6):803–20.

[23] Yan H, Parsons DW, Jin G, McLendon R, Rasheed BA, Yuan W, et al. IDH1 and IDH2 mutations in gliomas. N Engl J Med. 2009 Feb;360(8):765–73.

[24] Choi C, Ganji SK, DeBerardinis RJ, Hatanpaa KJ, Rakheja D, Kovacs Z, et al. 2-hydroxyglutarate detection by magnetic resonance spectroscopy in IDH-mutated patients with gliomas. Nat Med. 2012 Apr;18(4):624–9.

[25] Østergaard L. Principles of cerebral perfusion imaging by bolus tracking. J Magn Reson Imaging. 2005 Dec;22(6):710–7.

[26] Sourbron SP, Buckley DL. Classic models for dynamic contrast-enhanced MRI. NMR Biomed. 2013 Aug;26(8):1004–27.

[27] Welker K, Boxerman J, Kalnin A, Kaufmann T, Shiroishi M, Wintermark M. ASFNR Recommendations for Clinical Performance of MR Dynamic Susceptibility Contrast Perfusion Imaging of the Brain. AJNR Am J Neuroradiol. 2015.

[28] Aronen HJ, Gazit IE, Louis DN, Buchbinder BR, Pardo FS, Weisskoff RM, et al. Cerebral blood volume maps of gliomas: comparison with tumor grade and histologic findings. Radiology. 1994 Apr;191(1):41–51.

[29] Geer CP, Simonds J, Anvery A, Chen MY, Burdette JH, Zapadka ME, et al. Does MR Perfusion Imaging Impact Management Decisions for Patients with Brain Tumors? A Prospective Study. American Journal of Neuroradiology. 2011 Nov;33(3):556–562.

[30] Tofts PS, Kermode AG. Measurement of the blood-brain barrier permeability and leakage space using dynamic MR imaging. 1. Fundamental concepts. Magn Reson Med. 1991 Feb;17(2):357–67.

[31] Brix G, Kiessling F, Lucht R, Darai S, Wasser K, Delorme S, et al. Microcirculation and microvasculature in breast tumors: pharmacokinetic analysis of dynamic MR image series. Magn Reson Med. 2004 Aug;52(2):420–9.

[32] Sourbron S, Ingrisch M, Siefert A, Reiser M, Herrmann K. Quantification of cerebral blood flow, cerebral blood volume, and blood-brain-barrier leakage with DCE-MRI. Magn Reson Med. 2009 Jul;62(1):205–17.

[33] Patel P, Baradaran H, Delgado D, Askin G, Christos P, John Tsiouris A, et al. MR perfusion-weighted imaging in the evaluation of high-grade gliomas after treatment: a systematic review and meta-analysis. Neuro-Oncology. 2016 Aug;19(1):118–127.

[34] Heye T, Davenport MS, Horvath JJ, Feuerlein S, Breault SR, Bashir MR, et al. Reproducibility of dynamic contrast-enhanced MR imaging. Part I. Perfusion characteristics in the female pelvis by using multiple computer-aided diagnosis perfusion analysis solutions. Radiology. 2013 Mar;266(3):801–11.

[35] Tietze A, Mouridsen K, Mikkelsen IK. The impact of reliable prebolus T 1 measurements or a fixed T 1 value in the assessment of glioma patients with dynamic contrast enhancing MRI. Neuroradiology. 2015 Jun;57(6):561–72.

[36] Inglese M, Ordidge KL, Honeyfield L, Barwick TD, Aboagye EO, Waldman AD, et al. Reliability of dynamic contrast-enhanced magnetic resonance imaging data in primary brain tumours: a comparison of Tofts and shutter speed models. Neuroradiology. 2019 Aug;61(12):1375–1386.

[37] Vo HQ, Marwick TH, Negishi K. MRI-Derived Myocardial Strain Measures in Normal Subjects. JACC: Cardiovascular Imaging. 2018 Feb;11(2):196–205.

[38] Hayat TTA, Rutherford MA. Neuroimaging perspectives on fetal motor behavior. Neuroscience & Biobehavioral Reviews. 2018 Sep;92:390–401.

[39] Zhang S, Olthoff A, Frahm J. Real-time magnetic resonance imaging of normal swallowing. Journal of Magnetic Resonance Imaging. 2012 Jan;35(6):1372–1379.

[40] Buhmann-Kirchhoff S, Lang R, Kirchhoff C, Steitz HO, Jauch KW, Reiser M, et al. Functional cine MR imaging for the detection and mapping of intraabdominal adhesions: method and surgical correlation. European Radiology. 2008 Feb;18(6):1215–1223.

[41] Radmanesh A, Greenberg J, Chatterjee A, Smyth MD, Limbrick DD, Sharma A. Tonsillar Pulsatility Before and After Surgical Decompression for Children with Chiari Malformation type 1: An Application for True Fast Imaging with Steady State Precession. Neuroradiology. 2015 Apr;57(4):387–393.

[42] Sharma A, Parsons MS, Pilgram TK. Balanced steady-state free-precession MR imaging for measuring pulsatile motion of cerebellar tonsils during the cardiac cycle: a reliability study. Neuroradiology. 2012 Feb;54(2):133–138.

[43] Cousins J, Haughton V. Motion of the Cerebellar Tonsils in the Foramen Magnum during the Cardiac Cycle. American Journal of Neuroradiology. 2009 Sep;30(8):1587–1588.

[44] Strahle J, Muraszko KM, Kapurch J, Bapuraj JR, Garton HJL, Maher CO. Chiari malformation Type I and syrinx in children undergoing magnetic resonance imaging. Journal of Neurosurgery: Pediatrics. 2011 Aug;8(2):205–213.

[45] Taylor AJ, Salerno M, Dharmakumar R, Jerosch-Herold M. T1 Mapping. JACC: Cardiovascular Imaging. 2016 Jan;9(1):67–81.

[46] Marques JP, Kober T, Krueger G, van der Zwaag W, Van de Moortele PF, Gruetter R. MP2RAGE, a self bias-field corrected sequence for improved segmentation and T1-mapping at high field. NeuroImage. 2010 Jan;49(2):1271–1281.

[47] Schneider J, Kober T, Graz MB, Meuli R, Hüppi PS, Hagmann P, et al. Evolution of T1 Relaxation, ADC, and Fractional Anisotropy during Early Brain Maturation: A Serial Imaging Study on Preterm Infants. American Journal of Neuroradiology. 2016 Jan;37(1):155–162.

[48] Cho S, Jones D, Reddick WE, Ogg RJ, Steen RG. Establishing norms for age-related changes in proton T1 of human brain tissue in vivo. Magnetic Resonance Imaging. 1997;15(10):1133–1143.

[49] Steen RG, Ogg RJ, Reddick WE, Kingsley PB. Age-related changes in the pediatric brain: quantitative MR evidence of maturational changes during adolescence. AJNR American journal of neuroradiology. 1997 May;18(5):819–828.

[50] Eminian S, Hajdu SD, Meuli RA, Maeder P, Hagmann P. Rapid high resolution

T1 mapping as a marker of brain development: Normative ranges in key regions of interest. PLoS ONE. 2018 Jun;13(6):e0198250.

[51] Steenweg ME, Vanderver A, Blaser S, Bizzi A, de Koning TJ, Mancini GMS, et al. Magnetic resonance imaging pattern recognition in hypomyelinating disorders. Brain. 2010 Sep;133(10):2971–2982.

[52] Kamalian S, Kamalian S, Konstas AA, Maas MB, Payabvash S, Pomerantz SR, et al. CT Perfusion Mean Transit Time Maps Optimally Distinguish Benign Oligemia from True "At-Risk" Ischemic Penumbra, but Thresholds Vary by Post-processing Technique. American Journal of Neuroradiology. 2011 Dec;33(3):545–549.

[53] Uchitel OD, González Inchauspe C, Di Guilmi MN. Calcium channels and synaptic transmission in familial hemiplegic migraine type 1 animal models. Biophysical Reviews. 2013 Dec;6(1):15–26.

[54] Dannenberg F, Prager C, Schmidt F, Tietze A, Bittigau P, Kaindl AM. Intravenous Nimodipine Treatment for Severe Episode of ATP1A2 Hemiplegic Migraine. Pediatric Neurology. 2020 Nov;112:71–72.

[55] Schack VR, Holm R, Vilsen B. Inhibition of Phosphorylation of Na+,K+-ATPase by Mutations Causing Familial Hemiplegic Migraine. Journal of Biological Chemistry. 2012 Jan;287(3):2191–2202.

[56] Hansen MB, Tietze A, Haack S, Kallehauge J, Mikkelsen IK, Østergaard L, et al. Robust estimation of hemo-dynamic parameters in traditional DCE-MRI models. PLOS ONE. 2019 Jan;14(1):e0209891.

[57] Marquardt DW. An algorithm for least-squares estimation of non-linear parameters. J Soc Ind Appl Math. 1963;11(2):431–441.

[58] Hansen MB, Tietze A, Haack S, Kallehauge J, Mikkelsen IK, Østergaard L, et al. Robust estimation of hemo-dynamic parameters in traditional DCE-MRI models. PLOS ONE. 2019 Jan;14(1):e0209891.

[59] Schmid VJ, Whitcher B, Padhani AR, Taylor NJ, Yang GZ. Bayesian Methods for Pharmacokinetic Models in Dynamic Contrast-Enhanced Magnetic Resonance Imaging. IEEE Transactions on Medical Imaging. 2006 Dec;25(12):1627–1636.

[60] O'Hayon BB, Drake JM, Ossip MG, Tuli S, Clarke M. Frontal and Occipital Horn Ratio: A Linear Estimate of Ventricular Size for Multiple Imaging Modalities in Pediatric Hydrocephalus. Pediatric Neurosurgery. 1998;29(5):245–249.

[61] Yushkevich PA, Piven J, Hazlett HC, Smith RG, Ho S, Gee JC, et al. User-guided 3D active contour segmentation of anatomical structures: Significantly improved efficiency and reliability. NeuroImage. 2006 Jul;31(3):1116–1128.

[62] O'Rourke M, Gasperini R, Young KM. Adult myelination: wrapping up neuronal plasticity. Neural Regeneration Research. 2014 Jul;9(13):1261–1264.

[63] Hormuth DA, Sorace AG, Virostko J, Abramson RG, Bhujwalla ZM, Enriquez-

Navas P, et al. Translating preclinical MRI methods to clinical oncology. Journal of Magnetic Resonance Imaging. 2019 Mar;50(5):1377–1392.

[64] Tietze M, Schaumann A, Thomale U, Hofmann P, Tietze A. Dynamic cerebellar herniation in Chiari patients during the cardiac cycle evaluated by dynamic magnetic resonance imaging. Neuroradiology. 2019 May;61(7):825–832.

[65] Tietze A, Blicher J, Mikkelsen IK, Østergaard L, Strother MK, Smith SA, et al. Assessment of ischemic penumbra in patients with hyperacute stroke using amide proton transfer (APT) chemical exchange saturation transfer (CEST) MRI. NMR in Biomedicine. 2013 Nov;27(2):163–174.

[66] Blicher JU, Tietze A, Donahue MJ, Smith SA, Østergaard L. Perfusion and pH MRI in familial hemiplegic migraine with prolonged aura. Cephalalgia. 2015 May;36(3):279–283.

[67] Tietze A, Choi C, Mickey B, Maher EA, Ulhøi BP, Sangill R, et al. Noninvasive assessment of isocitrate dehydrogenase mutation status in cerebral gliomas by magnetic resonance spectroscopy in a clinical setting. Journal of Neurosurgery. 2017 Mar;128(2):391–398.

[68] Tietze A, Nielsen A, Klærke Mikkelsen I, Bo Hansen M, Obel A, Østergaard L, et al. Bayesian modeling of Dynamic Contrast Enhanced MRI data in cerebral glioma patients improves the diagnostic quality of hemodynamic parameter maps. PloS One. 2018;13(9):e0202906.

[69] of Neurological Disorders TNI, rt PA Stroke Study Group S. Tissue Plasminogen Activator for Acute Ischemic Stroke. New England Journal of Medicine. 1995 Dec;333(24):1581–1588.

[70] Wahlgren N, Ahmed N, Dávalos A, Hacke W, Millán M, Muir K, et al. Thrombolysis with alteplase 3–4Â·5 h after acute ischaemic stroke (SITS-ISTR): an observational study. The Lancet. 2008 Oct;372(9646):1303–1309.

[71] Wahlgren N, Ahmed N, Dávalos A, Ford GA, Grond M, Hacke W, et al. Thrombolysis with alteplase for acute ischaemic stroke in the Safe Implementation of Thrombolysis in Stroke-Monitoring Study (SITS-MOST): an observational study. The Lancet. 2007 Jan;369(9558):275–282.

[72] Hacke W, Kaste M, Bluhmki E, Brozman M, Dávalos A, Guidetti D, et al. Thrombolysis with Alteplase 3 to 4.5 Hours after Acute Ischemic Stroke. New England Journal of Medicine. 2008 Sep;359(13):1317–1329.

[73] Smith WS, Sung G, Starkman S, Saver JL, Kidwell CS, Gobin YP, et al. Safety and Efficacy of Mechanical Embolectomy in Acute Ischemic Stroke. Stroke. 2005 Jul;36(7):1432–1438.

[74] Berkhemer OA, Fransen PSS, Beumer D, van den Berg LA, Lingsma HF, Yoo AJ, et al. A Randomized Trial of Intraarterial Treatment for Acute Ischemic Stroke. New England Journal of Medicine. 2015 Jan;372(1):11–20.

[75] Goyal M, Demchuk AM, Menon BK, Eesa M, Rempel JL, Thornton J, et al.

Randomized Assessment of Rapid Endovascular Treatment of Ischemic Stroke. New England Journal of Medicine. 2015 Mar;372(11):1019–1030.

[76] Campbell BCV, Mitchell PJ, Kleinig TJ, Dewey HM, Churilov L, Yassi N, et al. Endovascular Therapy for Ischemic Stroke with Perfusion-Imaging Selection. New England Journal of Medicine. 2015 Mar;372(11):1009–1018.

[77] Campbell BCV, Majoie CBLM, Albers GW, Menon BK, Yassi N, Sharma G, et al. Penumbral imaging and functional outcome in patients with anterior circulation ischaemic stroke treated with endovascular thrombectomy versus medical therapy: a meta-analysis of individual patient-level data. The Lancet Neurology. 2019 Jan;18(1):46–55.

[78] Hjort N, Butcher K, Davis SM, Kidwell CS, Koroshetz WJ, Röther J, et al. Magnetic Resonance Imaging Criteria for Thrombolysis in Acute Cerebral Infarct. Stroke. 2005 Feb;36(2):388–397.

[79] Yuh WTC, Alexander MD, Ueda T, Maeda M, Taoka T, Yamada K, et al. Revisiting Current Golden Rules in Managing Acute Ischemic Stroke: Evaluation of New Strategies to Further Improve Treatment Selection and Outcome. American Journal of Roentgenology. 2017 Jan;208(1):32–41.

[80] Jokivarsi KT, Gröhn HI, Gröhn OH, Kauppinen RA. Proton transfer ratio, lactate, and intracellular pH in acute cerebral ischemia. Magnetic Resonance in Medicine. 2007;57(4):647–653.

[81] Law M, Yang S, Wang H, Babb JS, Johnson G, Cha S, et al. Glioma grading: sensitivity, specificity, and predictive values of perfusion MR imaging and proton MR spectroscopic imaging compared with conventional MR imaging. AJNR Am J Neuroradiol. 2003 Nov;24(10):1989–98.

[82] Khayal IS, Nelson SJ. Characterization of low-grade gliomas using RGB color maps derived from ADC histograms. J Magn Reson Imaging. 2009 Jul;30(1):209–13.

[83] Bulakbasi N, Kocaoglu M, Ors F, Tayfun C, Ucoz T. Combination of single-voxel proton MR spectroscopy and apparent diffusion coefficient calculation in the evaluation of common brain tumors. AJNR Am J Neuroradiol. 2003 Feb;24(2):225–33.

[84] Chang SM, Nelson S, Vandenberg S, Cha S, Prados M, Butowski N, et al. Integration of preoperative anatomic and metabolic physiologic imaging of newly diagnosed glioma. J Neurooncol. 2009 May;92(3):401–15.

[85] Verhaak RG, Hoadley KA, Purdom E, Wang V, Qi Y, Wilkerson MD, et al. Integrated genomic analysis identifies clinically relevant subtypes of glioblastoma characterized by abnormalities in PDGFRA, IDH1, EGFR, and NF1. Cancer Cell. 2010 Jan;17(1):98–110.

[86] Kickingereder P, Wiestler B, Graf M, Heiland S, Schlemmer HP, Wick W, et al. Evaluation of dynamic contrast-enhanced MRI derived microvascular permeability in recurrent glioblastoma treated with bevacizumab. Journal of Neuro-Oncology. 2014 Oct;121(2):373–380.

[87] Buchem MAv, Steens SCA, Vrooman HA, Zwinderman AH, McGowan JC, Rassek

M, et al. Global Estimation of Myelination in the Developing Brain on the Basis of Magnetization Transfer Imaging: A Preliminary Study. American Journal of Neuroradiology. 2001 Apr;22(4):762–766.

[88] Deoni SCL, Dean DC, O'Muircheartaigh J, Dirks H, Jerskey BA. Investigating white matter development in infancy and early childhood using myelin water faction and relaxation time mapping. NeuroImage. 2012 Nov;63(3):1038–1053.

[89] Löbel U, Sedlacik J, Güllmar D, Kaiser WA, Reichenbach JR, Mentzel HJ. Diffusion tensor imaging: the normal evolution of ADC, RA, FA, and eigenvalues studied in multiple anatomical regions of the brain. Neuroradiology. 2009 Apr;51(4):253–263.

[90] Watanabe M, Sakai O, Ozonoff A, Kussman S, Jara H. Age-related Apparent Diffusion Coefficient Changes in the Normal Brain. Radiology. 2013 Feb;266(2):575–582.

[91] Soun JE, Liu MZ, Cauley KA, Grinband J. Evaluation of neonatal brain myelination using the T1- and T2-weighted MRI ratio. Journal of Magnetic Resonance Imaging. 2017;46(3):690–696.

[92] Hagiwara A, Fujita S, Ohno Y, Aoki S. Variability and Standardization of Quantitative Imaging. Investigative Radiology. 2020 Mar;55(9):601–616.

[93] Sorace AG, Wu C, Barnes SL, Jarrett AM, Avery S, Patt D, et al. Repeatability, reproducibility, and accuracy of quantitative mri of the breast in the community radiology setting. Journal of Magnetic Resonance Imaging. 2018 Mar;48(3):695–707.

[94] Dekkers IA, Paiman EHM, de Vries APJ, Lamb HJ. Reproducibility of native T1 mapping for renal tissue characterization at 3T. Journal of Magnetic Resonance Imaging. 2018 Sep;49(2):588–596.

[95] Gracien RM, Maiworm M, Brüche N, Shrestha M, Nöth U, Hattingen E, et al. How stable is quantitative MRI? – Assessment of intra- and inter-scanner-model reproducibility using identical acquisition sequences and data analysis programs. NeuroImage. 2020 Feb;207:116364.

[96] Körzdörfer G, Kirsch R, Liu K, Pfeuffer J, Hensel B, Jiang Y, et al. Reproducibility and Repeatability of MR Fingerprinting Relaxometry in the Human Brain. Radiology. 2019 Aug;292(2):429–437.

[97] Tong Q, He H, Gong T, Li C, Liang P, Qian T, et al. Reproducibility of multi-shell diffusion tractography on traveling subjects: A multicenter study prospective. Magnetic Resonance Imaging. 2019 Jun;59:1–9.

[98] Galbraith SM, Lodge MA, Taylor NJ, Rustin GJ, Bentzen S, Stirling JJ, et al. Reproducibility of dynamic contrast-enhanced MRI in human muscle and tumours: comparison of quantitative and semi-quantitative analysis. NMR Biomed. 2002 Apr;15(2):132–42.

[99] Voelker MN, Kraff O, Brenner D, Wollrab A, Weinberger O, Berger MC, et al.

The traveling heads: multicenter brain imaging at 7 Tesla. Magnetic Resonance Materials in Physics, Biology and Medicine. 2016 Apr;29(3):399–415.

[100] Lundervold AS, Lundervold A. An overview of deep learning in medical imaging focusing on MRI. Zeitschrift für Medizinische Physik. 2019 May;29(2):102–127.

[101] Kickingereder P, Isensee F, Tursunova I, Petersen J, Neuberger U, Bonekamp D, et al. Automated quantitative tumour response assessment of MRI in neuro-oncology with artificial neural networks: a multicentre, retrospective study. The Lancet Oncology. 2019 May;20(5):728–740.

[102] Akkus Z, Galimzianova A, Hoogi A, Rubin DL, Erickson BJ. Deep Learning for Brain MRI Segmentation: State of the Art and Future Directions. Journal of Digital Imaging. 2017 Jun;30(4):449–459.

[103] Bernal J, Kushibar K, Asfaw DS, Valverde S, Oliver A, Martí R, et al. Deep convolutional neural networks for brain image analysis on magnetic resonance imaging: a review. Artificial Intelligence in Medicine. 2019 Apr;95:64–81.

[104] Cooper G, Hirsch S, Scheel M, Brandt AU, Paul F, Finke C, et al. Quantitative Multi-Parameter Mapping Optimized for the Clinical Routine. Frontiers in Neuroscience. 2020 Dec;14:611194.

Chapter 7

Acknowledgement

First of all, I want to express my thanks to Prof. Dr. med. Hamm, Prof. Dr. Med. Sci. Østergaard, Dr. med. Bohner, Prof. Dr. med. Liebig, and Prof. Dr. med. Kühn for their continuous support of my work. Their skilled advice, the allocation of necessary resources, and their financial support has made this thesis and the related publications possible.

I would like to thank Prof. Dr. med. Hamm, head of Charité Centrum für diagnostische und interventionelle Radiologie und Nuklearmedizin, for having created and maintaining a top Clinic for Radiology and Nuclear Medicine, of which I may be a part of. In addition to pioneering diagnostics and intervention, he provides an excellent academic and resourceful environment for my research and clinical activity.

My previous supervisor Prof. Dr. Med. Sci. Østergaard, Aarhus University, Denmark, is an exceptional scientist who has not only impressed me with his broad knowledge in natural and medical science, but also with his generosity and humanity. I was very lucky to be a part of his inspiring research team of engineers, physicists, medical doctors, and radiographers, without whom I would not have been able to accomplish this work.

After 20 years living and working in Denmark, Prof. Dr. med. Liebig, now at the Ludwig-Maximilians-Universität München, has offered me the position that still today is the dream of my professional life. He welcomed me unconditionally and played a very important role in introducing me into the academic and professional life at the Charité - Universitätsmedizin Berlin paving the way for this work.

The team at the Institute of Neuroradiology, Charité - Universitätsmedizin Berlin, maintained its notable strength under the new leadership of Dr. med. Bohner. I am very grateful to him and my colleagues for inspiring and professional discussions, for their flexibility, the incredible team spirit, and a good portion of humour. Dr. med. Bohner is extremely considerate and helpful. He has encouraged me continuously to pursue the work for this thesis and has cleared any obstacles out of my way.

Prof. Dr. med. Kühn has given me the one-time opportunity to take part in the Transregional Collaborative Research Center (SFB295RETUNE) that aims to investigate neuromodulation mechanisms in neurological disorders. Here, I have met visionary, helpful, and good-humoured colleagues who are not hesitant about any, in particular programming task, and have introduced me in an entire new and exciting research field. Funding by the Centre has also enabled me to finalise this work by granting me financial resources.

Both my research and clinical work would neither be meaningful nor successful without the contribution of numerous colleagues from the clinical disciplines. Here, I would like to express special thanks to the entire Dept. of Paediatric Neurosurgery, Charité - Universitätsmedizin Berlin, under the direction of Prof. Dr. med. Thomale. We have had many good conversations and the one or other cup of coffee together. Also, I wish to thank my colleagues from the Dept. of Paediatrics, Division of Neuropaediatrics as well as Oncology and Hematology, Charité - Universitätsmedizin Berlin, and especially Prof. Dr. med. Kaindl and PD Dr. med. Hernáiz Driever for the excellent and fruitful collaboration. From my previous affiliation at the Aarhus University Hospital, Denmark, out of many colleagues I would like to thank Dr. Gorm von Oettingen, PhD, Dept. of Neurosurgery, and Dr. med. Yasmin Lassen, PhD, Dept. of Neurooncology, as well as the whole team of the Dept. of Neuroradiology.

Neither my clinical nor research work could have been done without all the competent, patient, and efficient radiographers I have met throughout my professional life. None of the studies could have been performed without their valuable knowledge and I am grateful for having been able to learn numerous technical details. They have helped me with my research even in the fiercest clinical rush hours and together we have managed to convince many children to keep still in the scanner for yet another sequence. This leads me to my gratefulness towards all the patients who were willing to be part of my studies. Especially the patients affected by lethal brain tumours have often surprised me by their wish to contribute to research, even though their time is particularly precious.

Last but not least, I would like to thank my family for their unconditional support and for being so patient. I consider myself infinitely lucky to have them and, moreover, to be able to publish scientific work together with them.

Erklärung

§4 Abs. 3 (k) der HabOMed der Charité

Hiermit erkläre ich, dass

weder früher noch gleichzeitig ein Habilitationsverfahren durchgefürt oder angemeldet wurde,

die vorgelegte Habilitationsschrift ohne fremde Hilfe verfasst, die beschriebenen Ergebnisse selbst gewonnen sowie die verwendeten Hilfsmittel, die Zusammenarbeit mit anderen Wissenschaftlern/Wissenschaftlerinnen und technischen Hilfskräften sowie die verwendete Literatur vollständig in der Habilitationsschrift angegeben wurden,

mir die geltende Habilitationsordnung bekannt ist.

Ich erkläre ferner, dass mir die Satzung der Charité - Universitätsmedizin Berlin zur Sicherung Guter Wissenschaftlicher Praxis bekannt ist und mich zur Einhaltung dieser Satzung verpflichte.

Berlin, 05. September 2021